

Izmir Institute of Technology

The Graduate School

**ZEOLITE BASED COMPOSITES
IN ENERGY STORAGE**

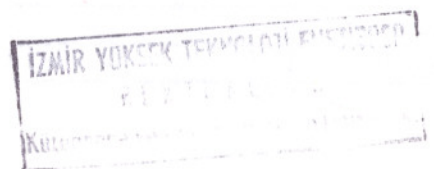
**A thesis in
Materials Science and Engineering**

**By
FİKİRİ NEGİŞ**

**Submitted in Partial Fulfillment
of the Requirements
for the degree of**

Master of Science in Materials Science and Engineering

March, 1999



We approve the thesis of Fikri NEGİŞ

Date of Signature

Prof. Dr. Semra ÜLKÜ

Supervisor

Department of Chemical Engineering

24.03.1999



Assoc. Prof. Dr. Zafer İLKEN

Department of Mechanical Engineering

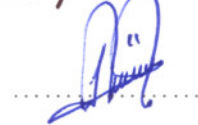
24.03.1999



Assist. Prof. Dr. Sacide ALSOY

Department of Chemical Engineering

24.03.1999



Prof. Dr. Muhsin ÇİFTÇİOĞLU

Head of Interdisciplinary

Material Science and Engineering Program

24.03.1999



ACKNOWLEDGEMENTS

I would like to thank Prof. Dr. Semra Ülkü and Asst. Prof. Selahattin Yılmaz for their supervision, help, support and encouragements they provided during this study.

I also would like to thank Prof. Dr. Muhsin Çiftçiođlu for his help and suggestions during the composite preparation, and Assoc. Prof. Dr. Zafer İlken for his help and contributions to the preparation of the experimental setup. Special thanks are to all research assistants for their contributions to this thesis, and to the laboratory technicians Nilgün Özgöl and Şerife Şahin for their help during the experimental work.

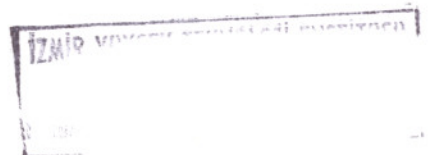
Finally, I would like to thank my family for their help and support and especially my father (I wish he was here) for his encouragements to apply for this Master of Science Program.

ABSTRACT

In this thesis, second phases were used for the zeolite-based composites with high thermal conductivity for energy storage applications. Natural zeolite, clinoptilolite received from large deposits in Turkey was used as matrix while aluminum, aluminum hydroxide and graphite were used as second phases for composite preparation.

Composites of different compositions (from 10 to 40 wt% additive loading) were prepared by mixing different amount of second phases to the clinoptilolite. Powder mixtures were pelletized using poly vinyl alcohol as a binder. The use of the binder was necessary to obtain mechanically strong pellets. The thermal treatment temperature and press pressure were determined as 150 °C and 60 bar for the pellet preparation. Powders were further characterized by thermogravimetric analysis, differential thermal analysis and differential scanning calorimetry. These characterizations have shown that three types of water is present in clinoptilolite: external water, loosely bound water and tightly bound water.

Thermal conductivities of these composite pellets prepared were determined using hot plate method. Thermal conductivity of pure matrix clinoptilolite pellets were measured as 0.26 W/mK. Thermal conductivity increased significantly by using aluminum as the second phase while it did not change much for graphite and aluminum hydroxide composites. For composites containing 40% aluminum or aluminum hydroxide or graphite, thermal conductivities of 1.18, 0.50, 0.43 W/mK were measured, respectively. Aluminum containing composites could be used as adsorbent bed materials and by this way, it may increase the performance of adsorption heat pumps.



ÖZ

Bu tezde enerji depolama uygulamaları için yüksek ısı iletkenlikli zeolit bazlı kompozitler çeşitli ikinci fazlar kullanılarak hazırlanmıştır. Türkiye’de fazlaca bulunan klinoptilolit matris olarak, alüminyum, alüminyum hidroksit ve grafit ikinci faz olarak kompozit hazırlamada kullanılmıştır.

Farklı kompozisyonlardaki kompozitler değişik miktarda ikinci fazlar ve klinoptolit karıştırılarak hazırlanmıştır. Karışım pelet haline getirilemediği için bağlayıcı madde olarak polivinil alkol kullanılmıştır. En iyi peletlerin (dağılmayan, çatlak içermeyen) 60 bar basınç altında yapılabildiği bulundu. Bu basınç altında hazırlanmış olan peletler 150 °C de ısı ı işlemden geçirilmiştir. Tozlar termal analiz cihazlarıyla (termogravitmetrik analiz, differensiyel termal analiz ve differansiyel taramalı kalorimetre) incelenmiş ve karakterize edilmiştir. Termal analiz sonuçları klinoptilolitde üç tür suyun bulunduğunu göstermiştir.

Hazırlanan peletlerin ısı iletkenlik katsayıları sıcak plaka metodu kullanılarak tayin edilmiştir. Klinoptolitin ısı iletkenlik katsayısı 0.26 W/mK olarak ölçülmüştür. Bu değer alüminyum tozunun kullanılmasıyla kayda değer bir şekilde artmış fakat grafit ve alüminyum hidroksit tozlarının kullanılmasıyla fazla artmamıştır. %40 alüminyum, grafit ve alüminyum hidroksit içeren kompozitlerin ısı iletkenlik katsayıları sırasıyla 1.18, 0.50 ve 0.43 W/mK olarak ölçülmüştür. Alüminyum içeren kompozitler adsorbent malzemesi olarak kullanılabilir ve bu yolla ısı pompalarının performansını artırabilir.

TABLE OF CONTENTS

LIST OF FIGURES	v
LIST OF TABLES	vii
I. INTRODUCTION	1
II. ADSORPTION AND ADSORBENTS	5
2.1 Physical and chemical adsorption	5
2.2 Adsorbents and adsorption equilibria	5
2.3 Zeolites	7
III. ADSORPTION IN ENERGY STORAGE	14
3.1 Adsorbent-adsorbate pair in the energy storage	14
3.2 Application of adsorption systems in energy storage	15
IV. DETERMINATION OF THERMAL CONDUCTIVITY	19
4.1 Hot wire method	19
4.2 Heat flow meter method	20
4.3 Hot plate method	21
V. COMPOSITE PREPARATION METHODS	23
VI. EXPERIMENTAL	25
6.1 Materials	25
6.2 Clinoptilolite powder preparation	25
6.3 Material characterization	25
6.4 Composite preparation	26
6.5 Determination of thermal conductivity	28
VII. RESULTS AND DISCUSSIONS	30
VIII. CONCLUSIONS	44
REFERENCES	46
APPENDIX	A1

LIST OF FIGURES

Figure 1	An $[AlO_4]$ or $[SiO_4]$ tetrahedra (primary building unit)	11
Figure 2	Secondary building unit classification	11
Figure 3	Air drying and heating system	17
Figure 4	Schematic diagram of a traditional compression refrigerator	18
Figure 5	Schematic diagram of a simple adsorption heat pump	18
Figure 6	An adsorption-desorption cycle for adsorption heat pumps	19
Figure 7	Schematic diagram of hot wire method setup	20
Figure 8	Variation of temperature with time	21
Figure 9	Variation of temperature with logarithmic time	21
Figure 10	Schematic diagram of heat flow meter method setup	22
Figure 11	Schematic diagram of hot plate method setup	23
Figure 12	Schematic view of the experimental setup	30
Figure 13	Variation of thermal conductivity with clinoptilolite composite loading	37
Figure 14	Densities of the composites versus clinoptilolite composite loading	39
Figure 15	DSC analysis of the clinoptilolite	40
Figure 16	DSC analysis of the clinoptilolite containing polyvinylalcohol	40
Figure 17	DSC analysis of the clinoptilolite and the clinoptilolite containing PVA	41
Figure 18	DSC analysis of the clinoptilolite and the all composites containing %20 additive	41
Figure 19	DTA analysis of the clinoptilolite and the clinoptilolite containing PVA	42
Figure 20	DTA analysis of the clinoptilolite and all the composites containing 20% additive	42
Figure 21	TGA analysis of the clinoptilolite and the clinoptilolite containing polyvinylalcohol	43

Figure 22 TGA analysis of the clinoptilolite, the clinoptilolite containing polyvinylalcohol and all the composites containing 20% additive	43
Figure 23 TGA analysis of the clinoptilolite	44
Figure 24 Particle size distribution of the clinoptilolite	A2
Figure 25 Particle size distribution of the aluminum hydroxide	A3
Figure 26 Temperature variation with respect to time for the clinoptilolite	A24
Figure 27 Temperature variation with respect to time for the clinoptilolite containing polyvinylalcohol	A24

LIST OF TABLES

Table 1	Zeolite based composite samples with additives	4
Table 2	Effective thermal conductivity and maximum adsorption capacity for zeolite based composites containing 40 % binders	4
Table 3	Particle sizes and thermal conductivities of glass beads, steel spheres and zeolite	5
Table 4	Classification of adsorbents according to their pore sizes	8
Table 5	Various physical properties of the clinoptilolite	14
Table 6	Clinoptilolite-based composites compositions	28
Table 7	Effect of PVA on the thermal conductivity of the clinoptilolite	34
Table 8	Variation of thermal conductivity with composite composition	35
Table 9	Thermophysical properties of selected materials	38
Table 10	Particle size analysis of the clinoptilolite	A2
Table 11	Particle size analysis of the aluminum hydroxide	A3
Table 12	Calibration data for thermocouple	A7
Table 13	Properties of aluminum	A1
Table 14	Properties of aluminum hydroxide	A1
Table 15	Properties of PVA	A1
Table 16	Properties of graphite	A1
Table 17	Thermal conductivity data for the clinoptilolite	A10
Table 18	Thermal conductivity data for the clinoptilolite containing PVA	A11
Table 19	Thermal conductivity data for the composite containing 10% aluminum	A12
Table 20	Thermal conductivity data for the composite containing 20% aluminum	A13
Table 21	Thermal conductivity data for the composite containing 30% aluminum	A14
Table 22	Thermal conductivity data for the composite containing 40% aluminum	A15
Table 23	Thermal conductivity data for the composite containing 10% graphite	A16
Table 24	Thermal conductivity data for the composite containing 20% graphite	A17
Table 25	Thermal conductivity data for the composite containing 30% graphite	A18

Table 26 Thermal conductivity data for the composite containing 40% graphite	A19
Table 27 Thermal conductivity data for the composite containing 10% aluminum hydroxide	A20
Table 28 Thermal conductivity data for the composite containing 20% aluminum hydroxide	A21
Table 29 Thermal conductivity data for the composite containing 30% aluminum hydroxide	A22
Table 30 Thermal conductivity data for the composite containing 40% aluminum hydroxide	A23

Chapter I

INTRODUCTION

In recent years, demand for energy has augmented as a result of increasing population and advancing up technology. With the depletion and the limited availability of energy sources, energy storage has gained importance in today's world [1, 2] .

Energy can be stored in several ways. More common ones are chemical, mechanical, electrical and thermal energy storage [2]. In general, energy storage systems involve the storage of energy in the same or another part of the system for later use.

Among the energy storage methods, thermal energy storage is the most attractive one. It has wide variety of applications in industry and can be stored in various ways as storage of sensible heat and as storage of latent heat. Methods for the latter includes: heat of fusion, heat of evaporation, heat of solution, heat of reaction and heat of adsorption [3-5] . Sensible energy storage is simple and cheap but requirement of large mass and volume of a storage material is an important problem. Some limitations appear in its application areas and to eliminate these limitations, combination of latent and sensible heat storage methods using heat of adsorption can be promising.

Heat of adsorption together with sensible heat in adsorption-desorption cycle depends mainly upon the availability of the appropriate adsorbent-adsorbate pairs. The criterions in choosing the pair can be outlined as:

1. Affinity of pair for each other (e.g., shape of isotherm, adsorption capacity)
2. Some thermal and transport properties of the pair (e.g., specific heat, thermal conductivity, diffusivity)
3. Degredation with cycling.

Moreover, materials used in energy storage should have suitable properties such as mechanical properties, long lifetime, low cost, availability, low mass and volume.

As an adsorbent, zeolite has been reported to be one of the most convenient energy storage materials, especially in adsorption-desorption cycle [6-9]. Zeolites are porous aluminosilicates of Group IA and Group IIA elements. Scientific interest and applications increased significantly after they were first discovered in 1756. Zeolites have some superior properties such as high ion-exchange capacity, high adsorption capacity and catalytic properties. They can adsorb large quantities of vapor, ranging from water vapor and ammonia to freons and carbon oxides, even at low partial pressures. On the other side, when they are heated they desorb most of the vapor even at high vapor pressures.

As it is described above, zeolites can be utilized in energy storage applications. There are several adsorbent-adsorbate pairs. Water-zeolite pair seems to be attractive for energy storage systems because of its high heat of adsorption, high adsorption capacity and high energy density.

Nowadays, zeolites are utilized in many applications and their use in energy storage have been investigated by many researches. Ülkü et al [5,10-16] investigated the use of zeolites in heat recovery and constructed various energy storage systems. Some possible application modes such as adsorption heat pumps were demonstrated

[10-12,14,15,17-20]. Advantages of the adsorption-desorption cycle were explained and characteristic properties of clinoptilolite (natural zeolite), [8,13,21] were also described. Moreover, theoretical analysis of several operating systems were compared with experimental results. Alefeld and his colleagues [17] studied various adsorption heat pumps as well as conventional heat pumps and described their performances. Some adsorption properties of zeolites related with the energy storage in thermodynamic systems were given by Restuccia et al [20,22,23]. Advantages of zeolite-water adsorption process were explained. Tchernev [18,19] investigated the principles of the zeolite adsorption heat pump and calculated cooling and heating efficiencies of the system related to adsorption-desorption cycle.

Although zeolites have very good adsorption properties, low heat transfer properties, especially low thermal conductivity of the zeolite pellet beds are the main drawbacks of adsorption thermal devices. These properties would limit the performance of an adsorption heat pump in relation with two coefficients: the

specific power and the coefficient of performance (COP). The former mainly depends on the size and the investment cost of the system and the latter is related with the energy efficiency and the operating cost of the system as indicated by Pino et al. [23]

Groll [24] studied the problems related to heat transfer enhancement inside the adsorbent bed. Experimental results of effective thermal conductivities (k_{eff}) for different adsorbent bed materials were reported. Highly porous metallic foams (Ni, Cu) forming porous blocks filled with 4A zeolites were shown to have higher effective adsorption bed thermal conductivity (1.7-8.3 W/mK) compared to 4A zeolite (0.36 W/mK). Highly porous metallic foams and fin like structures filled with metal hydrides improved k_{eff} giving a value of 4 W/mK. While metal hydrides containing 18 and 31 wt % Al powder had even higher k_{eff} , 11 and 23 W/mK respectively. Metal hydride compacts were stated to be short of anticipated specific power output breakthrough goal of 1 kW/kg. However, specific power outputs greater than breakthrough goal were stated to be within reach.

Pino et al. [23] studied the preparation of new composite materials, based on zeolite 4A with high thermal conductivity for heat pump applications. In the composite preparation, SiC, Si₃N₄ and graphite were used as additives and PTFE, Al(OH)₃ were used as binders. Composites were characterized in terms of equivalent thermal conductivity and maximum water adsorption capacity. To measure equivalent thermal conductivity, hot wire method was used. For comparison, an equivalent thermal conductivity of 0.09 W/mK for a zeolite bed was reported. Information about the samples prepared with PTFE binder and some high thermal conductivity additives are given in Table 1. The sample with only binder was considered as base case. It was observed that the additives slightly decreased the adsorption capacity probably due to the reduced amount of adsorbent material and porosity. In terms of equivalent thermal conductivity, graphite showed a reasonable increase whereas the addition of SiC and Si₃N₄ resulted in a slight decrease. Probably these two additives were very rigid and do not contribute to a mechanical contact between zeolite and the additive particle; on the other hand, graphite is a rather soft material which is likely to improve the equivalent thermal conductivity.

Table 1 Zeolite based composite samples with additives

PTFE (%)	SiC (%)	Si ₃ N ₄ (%)	Graphite (%)	Equivalent thermal conductivity, W/mK	Maximum Amount Adsorbed, wt%
10	0	0	0	0.15	21.30
10	10	0	0	0.15	19.70
10	0	10	0	0.12	20.05
10	0	0	10	0.18	18.90

The results obtained for zeolite based composites with 40 wt% binders containing are given in Table 2. The highest thermal conductivity and adsorption capacity was observed with samples prepared using aluminum hydroxide as the binder. A simple model was developed in order to compare composites in heat pump applications. Using this model, the influence of the effective thermal conductivity of a binder on the global heat transfer coefficient was examined. It was found that the highest global heat transfer coefficient was obtained with the composites bound with aluminum hydroxide. This produced an increase in the specific power of the adsorption heat pump from 100 W/kg obtainable with pelletized bed to a value of about 400 W/kg. Moreover, two component composite materials (zeolite + binder) were concluded to be preferable over three component materials composed of zeolite, binder and additive. [23]

Table 2 Effective thermal conductivity and maximum adsorption capacity for zeolite based composites containing 40 % binders

Binder type	Effective thermal conductivity, W/mK	Maximum Amount Adsorbed, wt %
PTFE	0.25	14.13
Graphite	0.36	14.74
Al(OH) ₃	0.43	23.27

Various possibilities and limits in heat transfer enhancement in adsorption beds were investigated by Guillemot and Gurgel [25,26]. They measured effective adsorbent bed thermal conductivities for binary mixtures of different sizes of adsorbent granulars of either glass beads, steel spheres or zeolite pellets and for

mixture of glass or zeolite adsorbents with Cu and Ni foams. The particle sizes and conductivities of adsorbent granulars are given in Table 3. The bed effective thermal conductivity was observed to increase by 26 % (from 0.09 to 0.113 W/mK) with bimodal mixture of zeolite particles containing 75 % coarse particles. The adsorbent type was observed to have a significant effect on thermal conductivity, i.e., steel spheres and glass beads provided effective thermal conductivities of 0.67 and 0.29 respectively. The copper foam and zeolite pellets mixture had a thermal conductivity 133 % greater than that of the zeolite bed alone. The use of metallic foam and and zeolite mixture in adsorbent beds was recommended.

Table 3 Particle sizes and thermal conductivities of glass beads, steel spheres and zeolite

	Glass Beads	Steel spheres	Zeolite
Coarse particles diameter, mm	10.0	10.25	4.0
Fine particles diameter, mm	1.5	2.04	0.5
Thermal conductivity, W/mK	0.93	20.0	0.18

Cacciola et al [24] tried to improve the heat transfer between a solid adsorbent material and a heat exchanger metal surface by providing a close contact with the metallic surface and the adsorbent bed, using adsorbents with different thermal conductivities. Therefore, different forms of the solid adsorbent were prepared. An organic binder, PTFE, was used with very fine zeolite powders in the preparation of the samples.

Sahnoune and Grenier [27] calculated the thermal conductivity of NaX zeolite pellets from measurements of the conductivity of a bed. Thermal conductivity of a glass bed in the presence of gases was also calculated in order to make a comparison. Thermal conductivity of the zeolite bed was calculated as 0.119 W/mK whereas it was 0.194 W/mK for the glass bed under the same conditions (in nitrogen atmosphere, at 200 mbar). Liu et al. [22] measured the thermal conductivity of zeolite brick using a simple and fast method based on transient conditions. Operation principle, the measurement conditions and the experimental device were described. The zeolite brick was prepared using a very fine 13X zeolite powder [28,29].

Thermal conductivity of clinoptilolite can be increased by the preparation of clinoptilolite-based composites which offers an advantage for improving the performance of the energy storage systems. In this study, zeolite based composites were prepared following powder route as a composite preparation method and aluminium, aluminium hydroxide and graphite were used as additives and polyvinyl alcohol (PVA) was used as a binder. The thermal conductivities of these composites were determined by using an experimental setup utilizing the hot plate method.

Chapter II

ADSORPTION AND ADSORBENTS

Adsorption involves the preferential partitioning of substances from the gaseous or liquid phase onto the surface of a solid substrate. The material in the adsorbed state is known as the adsorbate, as distinct from the adsorptive, i.e. the substance in the fluid phase which is capable of being adsorbed. [30,31]

Desorption is the reverse process of the adsorption, in which the adsorbed species are released back from the adsorbent to the surrounding.

2.1. Physical and Chemical Adsorption

There are two types of adsorption; physical (physisorption) and chemical adsorption (chemisorption). Physisorption involves mainly Van der Waals forces and electrostatic forces whereas chemisorption involves transferring and sharing of electrons between two phases; and a new chemical compound is formed as a result of chemical bond formation between the adsorbate and the outermost layer of the adsorbent.

Physical adsorption is a reversible process associated with low heats of adsorption. Chemical adsorption involves higher heats of adsorption and it is not reversible. Because, physisorption is very fast it reaches to equilibrium rapidly. [30,31]

2.2. Adsorbents and Adsorption Equilibria

2.2.1. Commercial adsorbents

Commercial adsorbents are porous substances possessing internal surface areas much greater than external surface areas; their total surface areas of them are almost equal to their internal surface areas. Adsorbents can be classified according to their pore sizes, pore volumes and surface areas. Classification of adsorbents according to their pore sizes is given in Table 4.

Table 4 Classification of adsorbents according to their pore sizes [5]

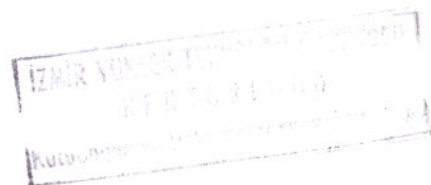
	Pore size
Micropores	$< \sim 20 \text{ \AA}^0$
Mesopores	$\sim 20 \text{ \AA}^0 - 500 \text{ \AA}^0$
Macropores	$> \sim 500 \text{ \AA}^0$

Activated carbon, silicagel, activated alumina and zeolites are common commercial adsorbents utilized in the industry.

Zeolites are crystalline alumina silicates of group I or II elements. They have uniform pore sizes ranging from 3 to 10 angstroms [5] and their regular pore structure makes them suitable for adsorption applications. They have a high internal surface area reaching to 800-1000 m²/gm [5]. They can adsorb polar and nonpolar molecules if proper conditions are provided. They can adsorb water vapor with high heat of adsorption even at very low concentrations. Activated carbon is an inert adsorbent material with a network of millions of microscopic channel-like pores. Under the microscope an activated carbon particle looks like a natural sponge perforated with countless small and very dense interconnecting channels. Conventional types of activated carbon generally have tridisperse pore structure (micropore, mesopore and macropore). Silicagel has a very large adsorption capacity especially for water. This ability is useful only at room temperatures but not at elevated temperatures. On the other hand, activated alumina has higher adsorption capacity than silicagel and it is generally used as a desiccant for drying applications.

2.2.2 Adsorption equilibria

Adsorption equilibria is a relationship between the adsorbent and the adsorbate. Amount of fluid adsorbed on a porous solid is determined by the temperature and the pressure of the surrounding media for the system under consideration. Experimental equilibrium data can be presented three different ways [5]:



-Adsorption Isotherms, the plot of amount adsorbed (x) as a function of equilibrium pressure (P) at constant temperature (T),

-Adsorption Isobars, the plot of amount adsorbed as a function of temperature at constant pressure,

-Adsorption Isosters, the plot of equilibrium pressure as a function of temperature at constant amount of gas or vapor adsorbed.

2.2.3 Heat of Adsorption

Heat of adsorption is defined as the heat evolved during the adsorption. Magnitude of heat is related to the contribution of electrostatic interactions in addition to the Van der Waals forces. The enthalpy change of the adsorbate on adsorption is denoted by ΔH . It is determined as 3.3 kcal/mole for argon adsorbate on LiX zeolite adsorbent. [7]

2.3. Zeolite

2.3.1. History

In 1756, Cronstedt, a Swedish mineralogist discovered the first zeolite, stillbite and made a classification of natural zeolites. He found that zeolites lose water rapidly when they are heated. For this reason, he used the Greek words “zeo” and “lithos” meaning stone that boils and called this material zeolite. [32]

In 1857, Damour [33] reported the hydration-dehydration properties of zeolites. In 1858, Eichhorn [34] showed some characteristic ion-exchange properties of zeolites. In 1925, Weigel and Steinhoff [35] demonstrated the separation of gas molecules on the basis of size by adsorption. In 1932, McBain [36] termed this phenomenon ‘molecular sieving’ and it became popular and is still used today. Until 1970’s adsorption and molecular sieving applications were studied and some new zeolite types were synthesized. In this period, some commercial applications were found and zeolites became an important industrial product. From 1970s to today, research on zeolites increased and their use in industrial applications have expanded.

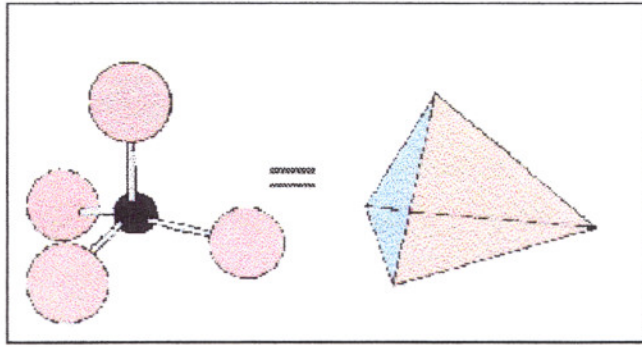


Figure 1 Primary building units of zeolite, $[AlO_4]$ or $[SiO_4]$ tetrahedra [6]

There are two different features in zeolites:

- 1) Internal pore system,
- 2) A system of uniform channels.

The former includes internal cage-like voids. In the latter, some channels are one-dimensional and others provide two- or three-dimensional channel systems by intersecting with similar channels.

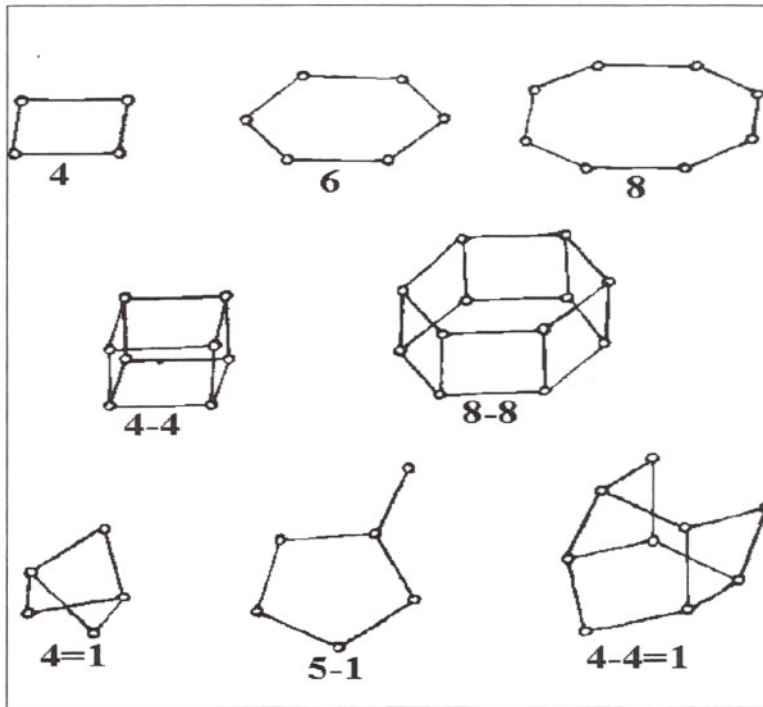


Figure 2 Secondary Building Unit Classification [9]

2.3.4. Adsorption and ion-exchange properties

Adsorption : Uniform pore size distribution of zeolites enables separations based on the molecular-sieve effect. This effect provides separation of materials according to differences in their molecular sizes. Size, shape and other properties like polarity of zeolites can provide sharp separations. As a result, zeolites selectively adsorb or reject molecules. [7,8]

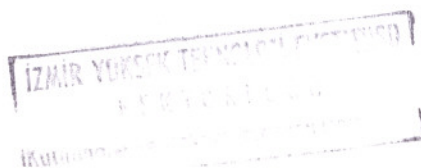
Electrostatic interactions are very important for an internal zeolite cavity. Also, there is a strong interaction between the zeolite and polar molecules such as water. In other words, zeolites possess a high affinity for water. Strong electrostatic field within the zeolite causes adsorption of non-polar molecules. In addition, crystal structure of these materials do not change after adsorbing or desorbing vapor. This property makes them applicable in some industrial applications like desiccation and energy storage. As a desiccant, zeolite is very effective in controlling moisture levels especially in low humidity ranges.

Zeolites have high heat of adsorption and ability to hydrate and dehydrate. These properties enable to use of zeolites in energy storage applications. Importance and the mechanism of energy storage processes using zeolites are explained in the following chapter.

Ion exchange : Since zeolites are porous, cations can move freely and migrate in and out of zeolite structures. The highly selective ion exchange capacity makes zeolites beneficial in controlling specific cationic levels in water systems, agriculture and in many other areas. [7]

2.3.5. Industrial Importance of Zeolites

Zeolites are widely used in the industry and they have many application areas such as waste water treatment and gas treatment[8]. They can also be used as livestock feed additives and for odor control in agriculture. Zeolites are utilized as adsorbents in oil industry and in energy storage applications such as heat pumps, heat transformer and refrigerator [11,12]. Moreover, they can also be used as water softeners in detergent builders replacing the undesired polyphosphate.



2.3.6. Natural Zeolites

Zeolite as a mineral was formed from deposition of ash from volcanoes in alkaline lakes many years ago. In other words, formation of the zeolite minerals can be explained as the natural alteration of volcanic ash in alkaline environments.

Some of the most common natural zeolites can be listed as:

- Analcime (Hydrated Sodium Aluminum Silicate)
- Chabazite (Hydrated Calcium Aluminum Silicate)
- Edingtonite (Hydrated Barium Aluminum Silicate)
- Epistilbite (Hydrated Calcium Aluminum Silicate)
- Erionite (Hydrated Sodium Potassium Calcium Aluminum Silicate)
- Goosecreekite (Hydrated Calcium Aluminum Silicate)
- Gmelinite (Hydrated Sodium Calcium Aluminum Silicate)
- Harmotome (Hydrated Barium Potassium Aluminum Silicate)
- Heulandite (Hydrated Sodium Calcium Aluminum Silicate)
- Laumontite (Hydrated Calcium Aluminum Silicate)
- Levyne (Hydrated Sodium Calcium Aluminum Silicate)
- Mesolite (Hydrated Sodium Calcium Aluminum Silicate)
- Mordenite (Hydrated Sodium Potassium Calcium Aluminum Silicate)
- Natrolite (Hydrated Sodium Aluminum Silicate)
- Phillipsite (Hydrated Potassium Sodium Calcium Aluminum Silicate)
- Scolecite (Hydrated Calcium Aluminum Silicate)
- Stellerite (Hydrated Calcium Aluminum Silicate)
- Stilbite (Hydrated Sodium Calcium Aluminum Silicate)
- Thomsonite (Hydrated Sodium Calcium Aluminum Silicate)

Natural zeolite, clinoptilolite was used in this work. Clinoptilolite is a silica-rich member of the heulandite family of natural zeolites and it is isostructural with the zeolite heulandite. Clinoptilolite and heulandite differ only in framework and exchange ion composition. Clinoptilolite represents the higher silica form of this structure and it was first discovered in the USA in the 1930s. Clinoptilolite occurs in large mineable deposits of relatively high purity in many parts of Turkey and the World.

Clinoptilolite can be colorless or white. It has glassy or silky luster. It is very stable towards dehydration and readily adsorbs water vapor and carbon dioxide. It is thermally stable is 700 °C in air. The general formula for clinoptilolite is:



Physical properties of clinoptilolite are given briefly in Table 5.

Table 5 Various physical properties of the clinoptilolite [7,13]

Density(kg/m ³)	967-1525
Si / Al ratio	4.25-5.25
Pore dimension (A ⁰)	(4.4 x 7.2), (4.1 x 4.7)
Thermal conductivity (W/mK)	0.185-0.606
Specific heat (kJ/kgK)	1.421
Void volume (%)	0.34

There are several application areas of clinoptilolite in industry: natural gas purification (removal of CO₂, H₂S, N₂ and H₂O), drying, air separation (both O₂ and N₂ production), flue gas clean up (SO₂ removal), and coal gasification (NH₃ removal).

It can also be used as an ion exchanger for ammonia, as a filler in paper industry, as a component of slow release fertilizers and soil conditioners, and as a dietary supplement in animal feedstock.

Chapter III

ADSORPTION IN ENERGY STORAGE

Adsorption-desorption cycle is one of the possible application modes to store energy.

Adsorption heat pumps (or refrigerators) and heat transformers are examples for energy storage applications. There are many factors which should be taken into account in energy storage including mass, volume and cost of the storage system as well as efficiency of the system. Among these factors, the choice of the most appropriate adsorbent-adsorbate combination is very important since it is the key part of the adsorption-desorption cycle.

3.1 Adsorbent-Adsorbate Pairs in The Energy Storage

The performance of a system utilizing an adsorption-desorption cycle mainly depends upon the availability of the proper adsorbent-adsorbate pair, the maximum capacity of the adsorbent for the adsorbate; amount of heat released during adsorption (heat of adsorption), affinity of the pair for each other (e.g., adsorption isotherms, isobars, isosters), boiling point of the adsorbate, latent heat of vaporization, heat capacity, thermal conductivity, mass diffusivity, ability for reactivation with the suitable energy source, cost and availability. Besides, operation temperatures like bed temperature, condenser and evaporator temperatures which change according to the specified design conditions also affects the performance of the system and should be considered in the choice the appropriate pair.

There are several adsorbent-adsorbate pairs including ammonium-calcium chloride, water-zeolite, methanol-active carbon, water-silica gel. Silica gel-water pair is suitable for low energy grade applications requiring low regeneration temperature. Methanol-zeolite or methanol-active carbon pairs can also be used for low temperature applications (lower than 0 °C).

The latent heat of water is very large compared to other adsorbates. Zeolite and water have high heat of adsorption with high adsorption capacity. These characteristic properties make zeolite-water pair superior for energy storage systems. Other

advantages of this pair are reversibility, negligible corrosiveness and constant volume during adsorption.

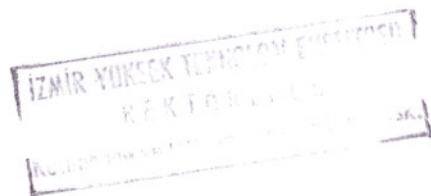
3.2. Application of Adsorption Systems in Energy Storage

Adsorption-desorption cycle can be utilized for storing energy for later use. Solar energy, waste heat, peak electricity and other sources of thermal energy can be recovered during the desorption process as latent heat and sensible heat, and then this recovered energy can be utilized efficiently during the adsorption process. Depending upon the principles of adsorption-desorption cycle some storage devices can be constructed easily and the systems including these devices can basically be classified in two groups: open and close cycle systems.

Open Cycle Systems

An adsorbent bed in which humid air is driven through is the key component in these systems. Since it is an exothermic process, heat is released during adsorption. As a result of the heat of adsorption, the temperature of the air increases., the Air possesses relatively high temperature and low humidity when it leaves the bed which can be utilized for drying processes and dessicant air conditioning.

The working principle of the open cycle is very simple as stated previously. Ülkü et al. [10,12,13,16] constructed several air drying and heating systems, two of the most common application modes of the open cycle system. The system shown in Figure 3 consists of an adsorption column (adsorbent bed) and an air conditioning section. The column was made of polyethylene pipe and consisted of two concentric cylinders. Thermocouples were placed into the column for temperature measurements and probes were installed for humidity measurements at the inlet and the outlet of the column.



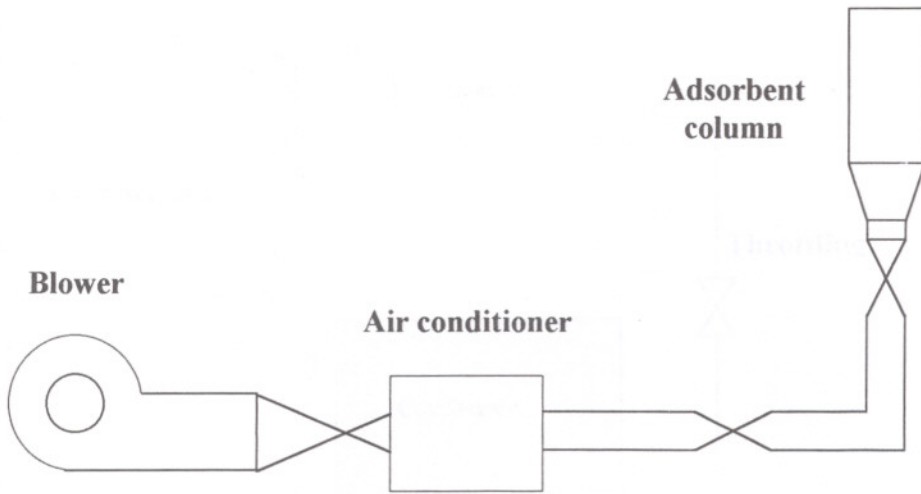


Figure 3 Air drying and heating system [7]

Close Cycle Systems

Heat pumps (or refrigerators) are devices for transferring heat from a low temperature source to a high temperature source by means of available energy sources.

Traditional thermodynamic systems such as compression refrigerators, shown in Figure 4, and the systems using adsorption cycle, shown in Figure 5, can be compared. The advantages of the adsorption-desorption cycle over the traditional heat pump systems can be given as:

1. Ability to operate with various energy sources (such as solar energy, geothermal energy, peak electricity),
2. Energy recovery and storage,
3. Lack of compressor and pumps,
4. High primary efficiency,
5. No vibration problems.

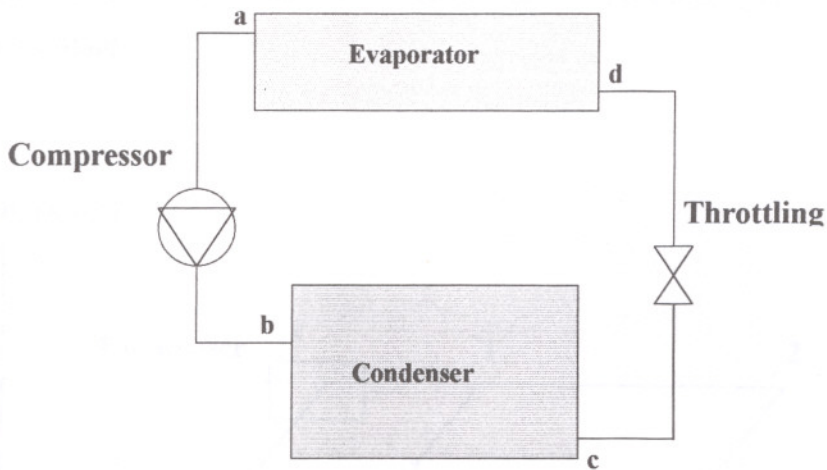


Figure 4 Schematic diagram of a traditional compression refrigerator

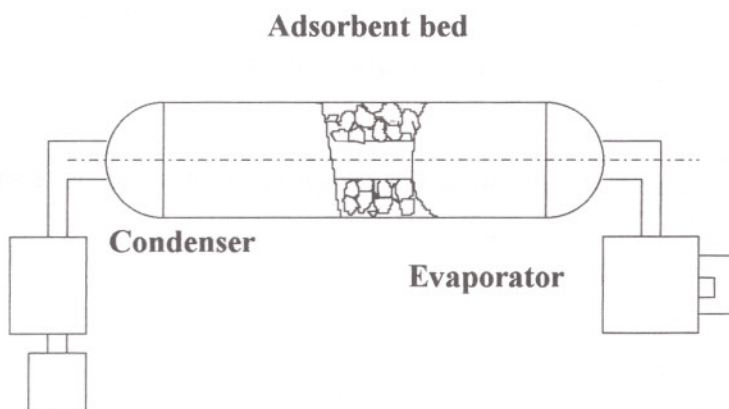


Figure 5 Schematic diagram of a simple adsorption heat pump [10]

An adsorption heat pump, shown in Figure 5, is a typical example for closed cycle systems and it consists of an adsorbent bed, a condenser and an evaporator.

Working principle of the cycle, shown in Figure 6, is very simple:

1-2 Isobaric heating and desorption: Adsorbent bed is heated at constant pressure desorbed vapor condenses in the condenser.

2-3 Isosteric cooling: Adsorbent bed is cooled down while the mass of the adsorbent remains constant.

3-4 Isobaric cooling and adsorption: The temperature of the adsorbent bed decreases while adsorbing the vapor coming from the evaporator.

4-1 Isosteric heating: Adsorbent bed is heated again while keeping the mass of the adsorbent constant.

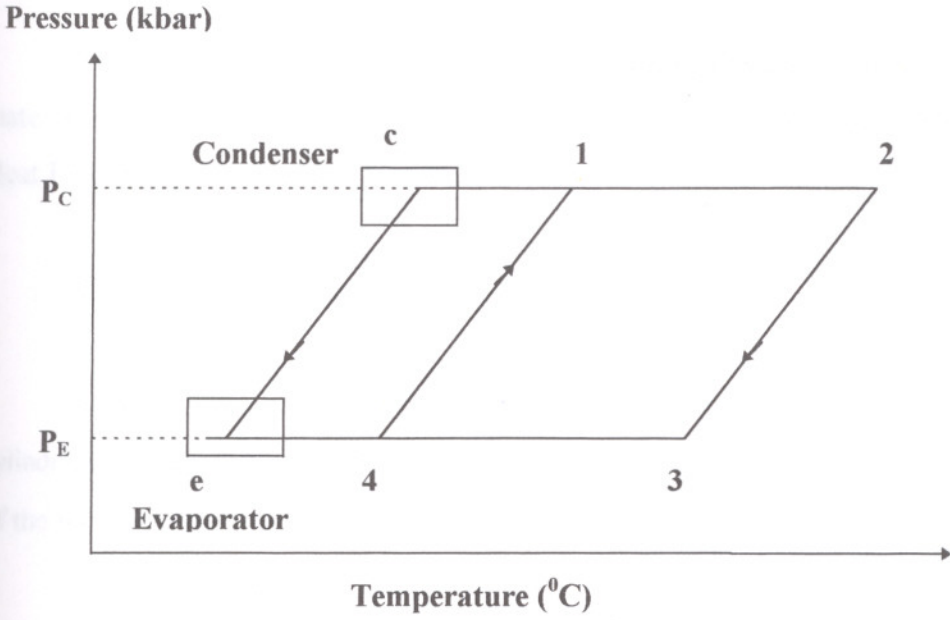


Figure 6 An adsorption-desorption cycle for adsorption heat pumps [10]

Chapter IV

DETERMINATION OF THERMAL CONDUCTIVITY

Several methods can be used for measuring thermal conductivities of materials. Methods commonly applied are considered here: Hot Wire Method, the Heat Flow Meter Method and Hot Plate Method.

4.1 Hot Wire Method

A heater wire is extended through the center of an endless homogeneous cylindrical sample at constant heat flux as shown in Figure 7 [37]. The temperature of the wire increases exponentially as given in equation 1 [22,38] and Figure 8:

$$T(r, t) = -\frac{q}{4\pi k} Ei\left(\frac{-r^2}{4at}\right) \quad 1$$

This equation was derived from the theory of heat transfer from a linear heat source in an infinite homogeneous mass as proposed earlier by Carslaw and Jaeger [38]. By expanding Ei in a power series and making some arrangements in this equation, a linear relationship can be obtained by converting time into logarithmic scale as shown in Figure 9. When greater linear angle is observed in this figure, it shows that the sample has low thermal conductivity.

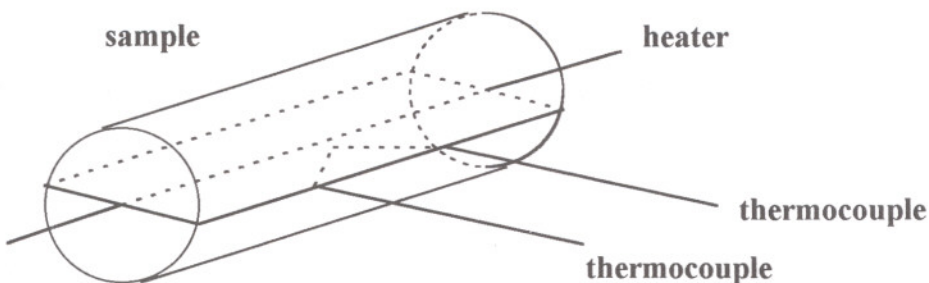


Figure 7 Schematic diagram of hot wire method setup

Thermal conductivity is determined at each time interval corresponding to a temperature increase using following equation[22]:

$$k = \frac{q \cdot \ln(t_2 / t_1)}{4\pi \cdot (T_1 - T_2)} \quad 2$$

where,

- k : thermal conductivity of sample (W/mK)
- q : thermal unit of heater per unit time and length (W)
- t₁, t₂ : time (second)
- T₁, T₂ : temperature at t₁ and t₂ (K)

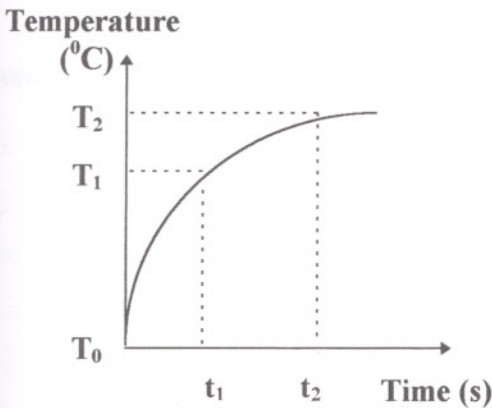


Figure 8 Variation of temperature with time

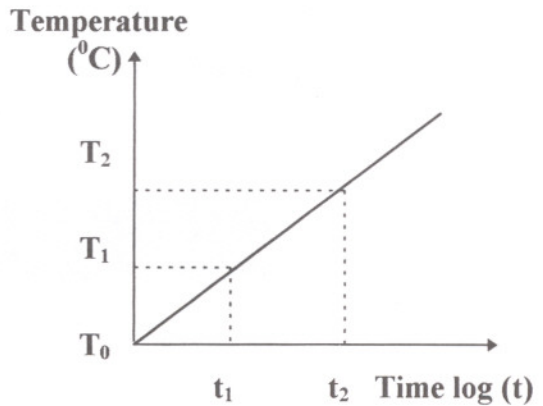


Figure 9 Variation of temperature with logarithmic time

Although hot wire method is a fast and simple method for thermal conductivity measurements, there are some sample size requirements. It must be infinitely long and thick. Size of the sample should not be small because heat loss to the surrounding will affect the measurement. Minimum required sample size depends on thermal conductivity of the sample, time for measurement and loaded thermal energy.

4.2 Heat Flow Meter Method

In heat flow meter method (Figure 10), sample is placed between two heated plates, each controlled at a different temperature [38,39]. Heat flows from the hot

plate to the cold plate and the thermocouples measure the temperature drop across the sample. Meanwhile, a sensitive transducer measures the heat flux in terms of voltage. After thermal equilibrium is established, thermal conductivity is determined from the Fourier's Law of Conduction [38,39]:

$$\frac{Q}{A} = \frac{k \cdot (T_h - T_c)}{d} \quad 3$$

where,

- Q/A : heat flux through the sample (W/m²)
- T_h-T_c: the hot and cold plate temperatures (K)
- d : sample thickness (m)

This method requires calibration with a material of known thermal conductivity to obtain a relation between the voltage and the heat flow.

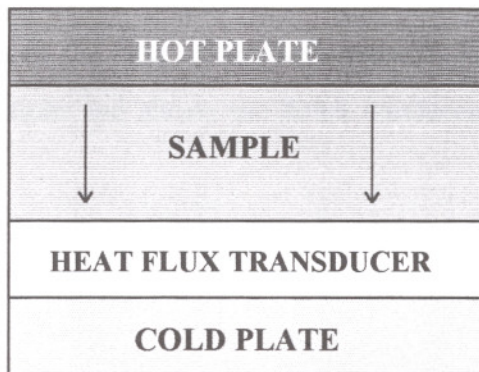


Figure 10 Schematic diagram of heat flow meter method setup

4.3 Hot Plate Method

Hot plate method setup consists of two identical samples, a main heater and two auxiliary heaters [40]. Each sample is placed between the main heater and auxiliary heater as illustrated in Figure 11. The main heater is kept at a higher temperature than auxiliary heaters whose temperatures should be the same.

Thermocouples measure the temperature drop across the sample. The heat flow through the sample is equal to the power supplied to the main heater. When

steady state conditions are established, thermal conductivity can be calculated using equation 3.

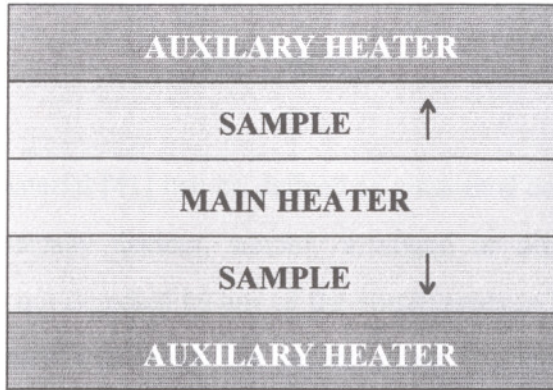


Figure 11 Schematic diagram of hot plate method setup

Among these measurement techniques, hot plate is the most practical and appropriate one for the determination of the thermal conductivity. Since there is no calibration requirement as in the case of heat flow meter method, there is no size limitation for the sample as in the case of hot wire method. Hot plate method is based on steady state conditions and allows the direct measurement of the thermal conductivity of a material.

Chapter V

COMPOSITES AND COMPOSITE PREPARATION METHODS

A composite material [41] can be defined as a material consisting of two or more physically and/or chemically distinct, suitably arranged or distributed phases. It has characteristics that are not depicted by any of the components in isolation. Generally, one component acts as a matrix in which the second phase is distributed. There are three commonly accepted types of composite materials:

1. Fibrous composites which consist of fibers in a matrix
2. Laminated composites which consist of layers of various materials
3. Particulate composites which are composed of particles in a matrix

Fibrous composites are composed of strong and stiff brittle fibers which are incorporated into a softer, more ductile matrix. The crystals are aligned in the fiber along the fiber axis. Moreover, there are fewer internal defects in fiber than in bulk material.

Laminated composites are composed of layers of different materials called laminates. Laminated composites are desirable when large surface area of the material are required. Lamination is used to combine the best aspects of the constituent layers in order to achieve a more useful material. The properties that can be emphasized by lamination are strength, stiffness, low weight, corrosion resistance, wear resistance, thermal insulation, acoustical insulation. Such claims are best represented by bimetal, laminated glass, plastic-based laminates, and laminated fibrous composites. They are inexpensive to manufacture and behave uniaxially (in-plane properties are different from out-of-plane or thickness direction properties).

Particulate composite materials contain a large number of randomly oriented particles. Consequently, particulate composites behave isotropically, i.e; the material properties are the same regardless of the direction along which they are measured.

Studies related to composite materials and their preparation have expanded since improvement of material properties is one of the basic purposes of material scientists.

Composite preparation methods can be classified in three groups: powder route, sol-gel route and reaction route. The most common one is the powder route. In this method materials are mixed and then hot pressed. The details of powder route related to this study is given in the following chapter. In the sol-gel route the composites are first mixed and gelled, then crushed, calcined and finally hot pressed. However, in the reaction route after mixing sintering is the next step. It is thermally treated to complete solid state reaction.

Chapter VI

EXPERIMENTAL

6.1 Materials

Natural zeolite used in this study was clinoptilolite obtained from Gördes, Turkey. The properties of the clinoptilolite is given in Table 5 in Chapter 3. PVA, purchased from Aldrich Chemicals Company, was used as the binder. The properties of this material can be found in Table 15 in Appendix A.1. Three different materials were used as second phases to prepare zeolite-based composites. These were aluminium, aluminium hydroxide, and graphite. The first two materials were received from Merck Limited Company and graphite from Aldrich Chemicals Company. The properties of these materials are given in Table 13, 14 and 16 in Appendix A.1, respectively.

6.2 Clinoptilolite Powder Preparation

Clinoptilolite powders were prepared from clinoptilolite particles having diameters less than 2 cm. These natural rock pieces were ground by a ball mill for 4 hours. The details of the milling operation is given in Appendix A.2. Powders obtained from the ball mill was dried at 65⁰C and sieved through a 45 µm sieve. This powder was used as the matrix in the preparation of composites.

6.3 Materials Characterization

Clinoptilolite was characterized by ASAP 2010 Accelerated Surface Area and Porosimetry System in which nitrogen was used as the adsorptive gas at liquid nitrogen temperature. Degassing was done at 350 ⁰C and surface properties of the clinoptilolite were determined using volumetric method. BET surface area and Langmuir surface area were determined as 47.4 m²/gr and 55.3 m²/gr, respectively. Both surface areas have the same correlation coefficient of 0.999.

Materials used in composite preparation were characterized in the particle size analyzer (Malvern Instruments Ltd.). Particle size analysis results of the clinoptilolite powder is given in Table 10 and Figure 24 in Appendix A2 and

aluminum hydroxide as given in Table 11 and Figure 25 in Appendix A3. Average mean particle diameters were determined as 15.91 and 24.26 μm , respectively. Agglomeration might have affected this particle size analysis results. On the other hand, as graphite and aluminum are very fine powders, it was not possible to determine their particle sizes. Particle size of the graphite was reported to be 1-2 μm by the chemical company.

Thermal behaviour of the clinoptilolite and the composites were investigated by Thermogravimetric Analyzer (TGA), Differential Scanning Calorimeter (DSC), and Differential Thermal Analyzer (DTA). Thermal analysis measurements (Shimadzu Thermal Analyze Instruments) were performed on clinoptilolite, clinoptilolite-PVA and the clinoptilolite-based composites containing %20 second phases. Heating rate was kept constant at 10 $^{\circ}\text{C}/\text{min}$ in all the analyses. Nitrogen was used as the adsorptive gas during the analysis and its flow rate was 15 ml/min for TGA and 20 ml/min for DTA and DSC.

Thermal conductivities of the clinoptilolite, clinoptilolite-PVA and the prepared composites were determined by using the experimental setup for thermal conductivity which was described previously in section 6.5.

6.4 Composite Preparation

Clinoptilolite composites with different compositions were prepared by using varying amounts of aluminium, aluminium hydroxide and graphite powders as second phases. They were labelled in terms of composite components weight ratio, as given in Table 6. The composite preparation procedure consisted of three steps:

1. The preparation of mixtures of zeolite, binder and second phase powders
2. Pellet preparation
3. Thermal treatment

Cracks and defects were observed in the pellets when they were prepared without using a binder. Therefore, PVA was added as the binder since it has a binding effect and it distributes inorganic molecules in composite materials. PVA was added to clinoptilolite in such an amount that would give a 3% mass ratio of

PVA. PVA was dissolved in distilled water by heating up to 60 °C. The solution obtained was added to the clinoptilolite and thoroughly mixed. This suspension was then dried at about 70 °C to have 3% PVA in the clinoptilolite.

Aluminium, aluminium hydroxide and graphite powders were added to the clinoptilolite containing 3% PVA in varying amounts to get different zeolite composite compositions. The mixture were then homogenized by stirring.

Table 6 Clinoptilolite-based composites compositions

Samples	Zeolite + PVA	Al	Al(OH) ₃	Graphite
	%	%	%	%
A1	90	10	—	—
A2	80	20	—	—
A3	70	30	—	—
A4	60	40	—	—
B1	90	—	10	—
B2	80	—	20	—
B3	70	—	30	—
B4	60	—	40	—
C1	90	—	—	10
C2	80	—	—	20
C3	70	—	—	30
C4	60	—	—	40

The mixtures were pressed by hydraulic press in order to obtain clinoptilolite-based pellets having a circular disc shape. The hydraulic press pressure reading should be converted to the real pressure applied to the die. Small pressures about 20 bar were not enough to create intact composites whereas large pressures (e.g., 100 and 120 bar), were excessive, and causing defects and cracks in the composites. This showed that pressure was an important parameter in pellet

preparation and a press pressure of 60 bar was found to be the optimum value for the composite preparation.

After drying the pellets prepared at 150°C for 2 hours, their thermal conductivities were measured.

6.5 Determination of Thermal Conductivity

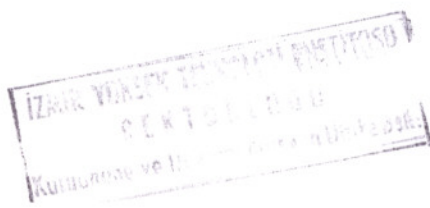
The experimental setup based on hot plate method was used for determination of thermal conductivities of the pellets. A schematic diagram of the setup is shown in Figure 12. Each experimental uses two composite pellets, four copper discs, four thermocouples, DC power supply and a data acquisition device (datalogger).

Diameter and thickness of the pellets were about 46 and 4 mm, respectively. The copper discs had the same diameter as pellets.

The setup could be considered in two symmetric parts. In each part, one pellet was sandwiched between two copper discs having different thicknesses (10 and 15 mm). Two heaters connected to the DC power supply were installed between these two parts (copper-pellet-copper). Constant and equal heat fluxes were given to the system to ensure stability.

The specimen surfaces were grooved at one location to locate the thermocouples for the accurate temperature measurements. In order to minimize heat losses and promote one dimensional heat flow, the whole system was wrapped with polyethylene foam insulation. Silicon grease was used to fill the air gap between the copper discs and the pellet to eliminate the effect of contact resistance.

Datalogger collected the temperatures measured from the K type thermocouples located at both sides of the specimens. Because, the accuracy of the temperature measurement has a significant effect on the estimation of the thermal conductivity thermocouples were calibrated, as described in Appendix A.4. Thermocouple locations and the cross-sectional view of the experimental setup are also illustrated in Figure 12. Temperature data which are given with related figures in Appendix A.5. were obtained at one minute intervals. Temperatures measured after reaching steady state were used to calculate thermal conductivity of the composites using Equation 3.



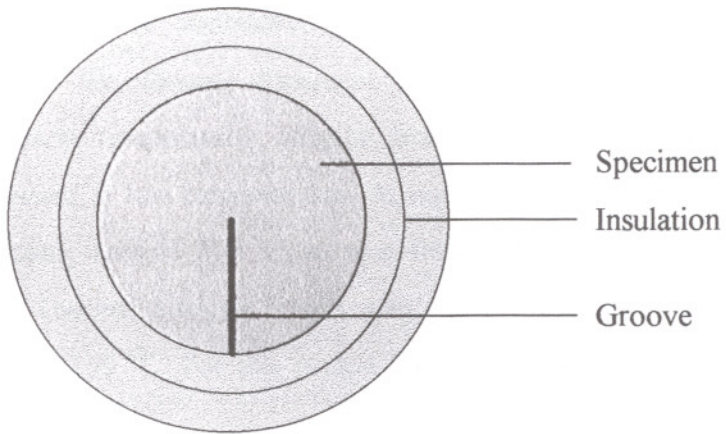
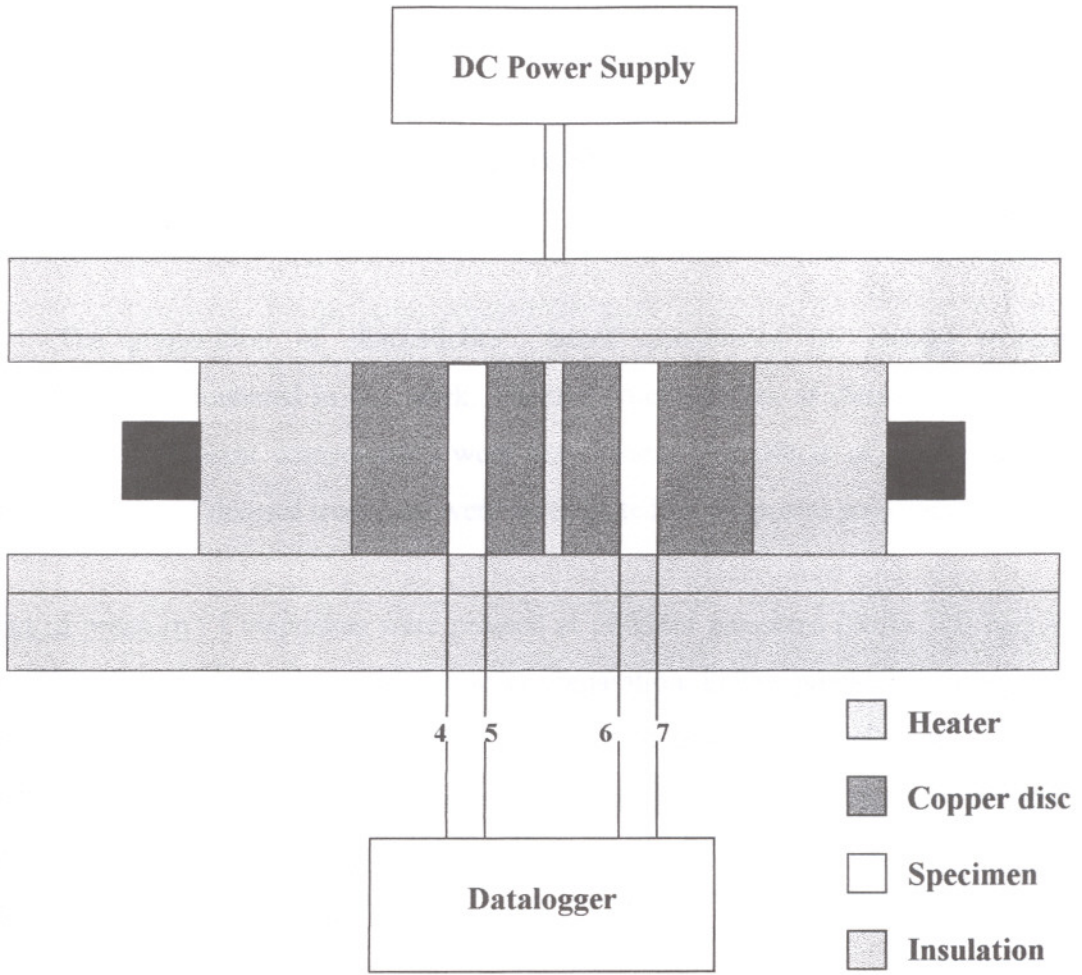


Figure 12 Schematic view of the experimental setup

TEKNIK YUKSEK TEKNOLOGI ENSTİTÜSÜ
 FEN BİLİMLERİ ENSTİTÜSÜ
 Kütüphane Yeri: ...

Chapter VII

RESULTS AND DISCUSSIONS

The preparation of clinoptilolite based composites for energy storage applications was examined in this work. Thermal conductivities of clinoptilolite based composites of different compositions were determined. The effects of press pressure and temperature of thermal treatment were investigated in composite preparation.

Effect of pressure : Composites were pressed at different pressures (20 to 120 bar) in order to find the optimum pressure for pellet preparation. Pellets prepared at low press pressures were not intact. Cracks and defects were observed in the pellets when large pressures were applied. After a few trials, the optimum press pressure of 60 bar was found to be suitable for pellet preparation. This pressure was further used in the pellet preparation.

Effect of thermal treatment : Thermal treatment is required for the composites prepared to ensure thermal stability. Since composites contain additives and the binder; their thermal behaviour should also be considered in choosing the thermal treatment temperature. To determine the thermal treatment temperature, composites were thermally treated at different temperatures ranging from 80 °C to 200 °C. Intact composites were not obtained at low temperatures. At higher temperatures aluminium hydroxide starts decomposing around 200 °C, as seen from thermal analysis given in Figures 18, 20 and 22. Thermal analysis results also showed that composites lost almost all external water by 150 °C. For this reason, this was chosen as an optimum thermal treatment temperature.

Thermal Analysis of the Samples

Powder mixtures used for composite preparation were characterized by DSC, DTA and TGA thermal analysis methods. The water content of clinoptilolite, clinoptilolite-PVA and particle mixtures used for the composites containing 20% additives were brought to the same relative humidity (around 75 %) by keeping in a desiccator containing NH_4Cl solution for a day. These samples were then used in thermal analysis.

Initially, DSC analyses were performed to determine the changes taking place in the samples with temperature. These results are given in Figures 15,16, 17 and 18. Clinoptilolite sample showed an endothermic peak between temperatures of 54 and 148 $^{\circ}\text{C}$. Clinoptilolite containing PVA gave an endothermic peak between temperatures of 54 and 171 $^{\circ}\text{C}$. From these figures, heat of dehydration for clinoptilolite and clinoptilolite containing PVA were calculated as 47.22 kJ/kg and 52.58 kJ/kg, respectively. The shift between the two peaks was probably due to the decomposition of PVA. Clinoptilolite containing PVA was considered as the reference material in this study.

DSC analysis of clinoptilolite, clinoptilolite-PVA and the composites containing 20% additives are given in Figure 18. An endothermic peak was observed for all samples. This peak refers to the dehydration of the sample. The peak areas were smaller for the samples containing aluminum and graphite. This indicated that water desorption was decreased by the addition of these materials. Since graphite and aluminum are hydrophobic and non porous, it might have caused the reduction in amount of water desorbed. On the other hand, the sample containing $\text{Al}(\text{OH})_3$ gave an endothermic peak similar to the clinoptilolite at approximately the same temperature but the peak area was larger than the clinoptilolite indicating that heat of dehydration was higher for $\text{Al}(\text{OH})_3$. Another endothermic peak was observed for this sample at temperatures between 236 and 357 $^{\circ}\text{C}$ which was considered to be due to the decomposition of aluminum hydroxide.

Similar trends with DSC were obtained in DTA analysis of clinoptilolite and clinoptilolite-PVA, as given in Figure 19. Endothermic peaks at 35 and at 648 $^{\circ}\text{C}$ and

an exothermic peak at 826 °C were observed for clinoptilolite. This endothermic peak indicated the destruction of clinoptilolite sample. For clinoptilolite-PVA, a slight change was observed in peak temperatures with respect to the clinoptilolite. These two samples and the composites containing 20% additives were compared in Figure 20. The results were consistent with DSC analysis. The same endothermic peak for the composite containing 20% aluminum hydroxide was observed around 300 °C. The exothermic peaks were observed around 830 °C for clinoptilolite, clinoptilolite-PVA and the sample containing aluminum hydroxide. However, these peaks were not observed for the remaining two samples. In addition, two endothermic peaks were observed around 1100 °C for these two samples. This might be due to the residual oxygen remaining in the samples.

In Figure 21, TGA analysis of clinoptilolite and clinoptilolite-PVA are given. Both samples showed the same thermal behaviour up to 230 °C. Addition of PVA shifted the clinoptilolite curve after this temperature which might be due to the PVA decomposition. No significant desorption of water occurred above 600 °C for both samples. 14.22% and 16.41% weight losses were obtained at 1000 °C for clinoptilolite and clinoptilolite-PVA, respectively. In Figure 22, TGA analysis of clinoptilolite, clinoptilolite-PVA and the samples containing 20% additive are shown. Up to 230 °C all samples showed similar curves. However, after this temperature, the composite containing aluminum hydroxide showed a significant shift in the TGA curve. This was due to the decomposition of the aluminum hydroxide which was consistent with both DSC and DTA analyses. A slight increase in weight loss was observed around 900 °C due to the presence of aluminum in the sample. Possible nitrides formation might have caused this increase. The highest weight loss was observed in the sample containing graphite. 11.34% and 19.99% weight losses were obtained for the samples containing 20% aluminum and aluminum hydroxide, respectively.

To examine thermal behaviour of clinoptilolite easily, its TGA analysis is also given in Figure 23. Inflection points on TGA curve was used to determine the boundaries of different types of water. Three kinds of water was observed in zeolites: external water, loosely bound water and tightly bound water. External water region was

around 80 °C. Loosely bound water region was between 86.72 °C and 271.40 °C. Tightly bound water region started from 271.40 °C. In this analysis, distinguishing the region of loosely and tightly bound water was difficult. Knowlton et al. [39] reported these two temperatures as 80 and 170 °C. The differences may be due to the analysis conditions and the sample properties.

Thermal Conductivity Measurements

Thermal conductivities measured for pure clinoptilolite and the clinoptilolite containing the binder, PVA, are given in Table 7. Ülkü et al. measured thermal conductivity as 0.185 W/mK for compacted clinoptilolite powders from Bigadiç [13]. Addition of 3 % PVA to clinoptilolite increased thermal conductivity slightly. This could be because of the binding effect and low content of PVA in clinoptilolite. Pino et al. [23] prepared zeolite 4A composites using PTFE as a binder. They reported that thermal conductivity of the 4A zeolite changed very little with the binder content. This was in agreement with the results given here.

Table 7 Effect of PVA on the thermal conductivity of the clinoptilolite

Sample	Thermal Conductivity (W/mK)
Clinoptilolite	0.26
Clinoptilolite + PVA	0.29

Thermal conductivities measured for composites with different compositions are given in Table 8. They are also plotted in Figure 13. When 10% graphite was added to the clinoptilolite-PVA a small increase (10%) was obtained in thermal conductivity. As percentage of graphite loading increased thermal conductivity values increased slightly. It increased from 0.32 to 0.42 by changing graphite content from 10 to 30 %. Addition of 30% graphite increased the thermal conductivity by 48% compared to the reference material. At higher loading, thermal conductivity remained almost constant. This slight increase at lower graphite contents might be due to the formation of interconnected

graphite network which favors heat transfer as graphite has a thermal conductivity of 5.70 W/mK [43] . Because graphite powder used in the composites had very small particle sizes (1-2 μm), mechanical contact between the particles may increase heat transfer. Layer orientation of the graphite is reported [23] to have a significant affect on the thermal conductivity of the composites with the applied pressure direction. Since graphite is an isotropic material, thermal conductivity of the final composite obtained would be different according to the direction of pressure applied. Thermal conductivities of 0.18, 0.26, 0.34 and 0.36 W/mK were reported for the zeolite 4A composites containing 10%, 20%, 30% and 40% graphite respectively [23]. These were close to the measurements obtained in this study.

Table 8 Variation of thermal conductivity with composite composition

Sample name	Al%	Al(OH) ₃ %	Graphite%	k (W/mK)
A1	10	—	—	0.45
A2	20	—	—	0.59
A3	30	—	—	0.88
A4	40	—	—	1.18
B1	—	10	—	0.38
B2	—	20	—	0.43
B3	—	30	—	0.49
B4	—	40	—	0.50
C1	—	—	10	0.32
C2	—	—	20	0.39
C3	—	—	30	0.42
C4	—	—	40	0.43

Thermal conductivities of the composites containing aluminum hydroxide did not change significantly with aluminum hydroxide loading. By increasing loading from 10 to 40 %, thermal conductivity increased from 0.38 to 0.50 W/mK. It remained

nearly constant above 30 % loading. An increase of 72% in thermal conductivity compared to the reference material was obtained. This might be the result of a good mechanical contact between the particles provided by aluminum hydroxide. As mean diameters of the aluminum hydroxide particles (24.26 μm) were greater than mean diameters of clinoptilolite (15.91 μm), clinoptilolite particles provided better contact by filling empty spaces between the aluminum hydroxide particles. No reported data on thermal conductivity of $\text{Al}(\text{OH})_3$ was found in literature. However, its thermal conductivity would be higher than clinoptilolite. Thermal conductivity results measured were close to the one reported by Pino et al [23] for zeolite 4A containing $\text{Al}(\text{OH})_3$. They measured thermal conductivities of 0.25, 0.35, 0.43 and 0.43 W/mK for composites containing 10%, 20%, 30% and 40% aluminum hydroxide respectively.

The change in thermal conductivities measured for different aluminium hydroxide and graphite loadings were very close to each other. Slightly higher thermal conductivity values were obtained with respect to the composites containing graphite.

Addition of aluminum to the clinoptilolite-PVA increased thermal conductivity significantly. As percentage of aluminum loading increased thermal conductivity increased linearly as shown in Figure 13. Thermal conductivity increased from 0.45 to 1.18 W/mK by changing aluminum content from 10% to 40%. Higher increases in thermal conductivity might be due to its high thermal conductivity (237 W/mK) [40]. In addition, aluminum powder had a platey structure. This might also be effective in increasing thermal conductivity.

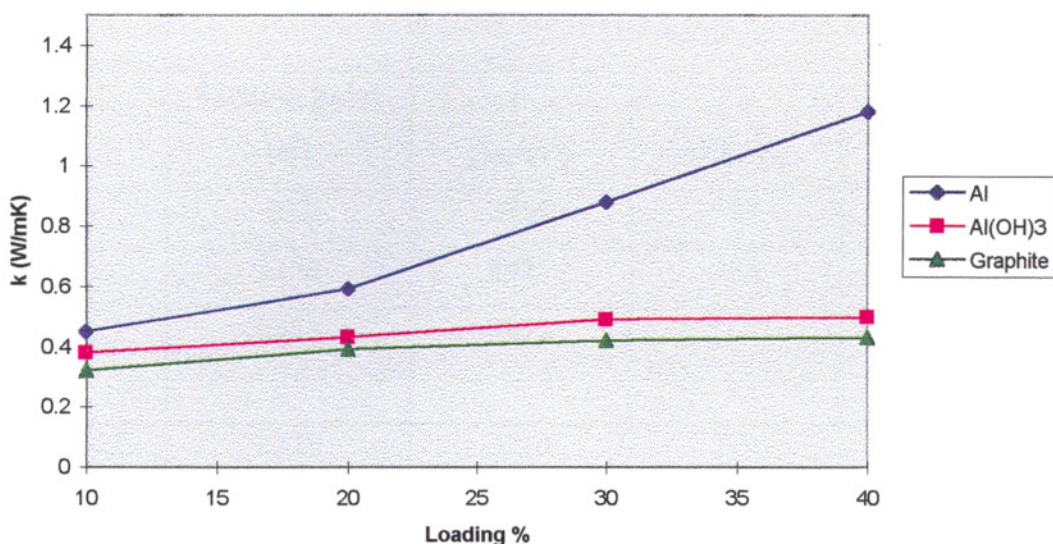


Figure 13 Variation of thermal conductivity with clinoptilolite composite loading

Thermal conductivities of the second phases on their own as pellets were attempted to be measured in order to make comparison between these materials and all the composites prepared. However, cracks and defects were observed in the pellets prepared by the second phase materials. Therefore, PVA was added to these materials to obtain intact pellets. It was possible to prepare the pellets of graphite and aluminum containing PVA. However, PVA was not effective for aluminum hydroxide containing PVA to obtain an intact pellet. Therefore, only thermal conductivities of graphite and aluminum pellets could be measured. However, the datalogger in the experimental set was not able to measure temperature drops less than 0.01 °C. Consequently, their thermal conductivities were not determined. Since there were no available data for the additives used in the composite preparation, thermophysical properties of some selected materials are given in Table 9.

Handwritten text and stamps at the bottom of the page, including a circular stamp and some illegible markings.

Table 9 Thermophysical properties of selected materials

Composition	Melting point (K)	Properties at 300 K		
		ρ (kg/m ³)	C_p (J/kgK)	k (W/mK)
Aluminum	933	2702	903	237
Copper	1358	8933	385	401
Aluminumoxide, sapphire	2323	3970	765	46
Graphite, pyrolytic	2273	2210	709	
k , // to layers				1950
k , \perp to layers				5.70

Determination of thermal conductivities of the composite materials is a complex problem as it is affected by many factors such as composition, porosity, shape, size, uniformity, particle size, particle content and density. Particularly porosity may have a dramatic influence on the thermal conductivity. Therefore, further studies could help to have better understanding of thermal conductivity of these composite materials.

Adsorption properties of the adsorbent is also important for energy storage systems and it should have been characterized. However, no adsorption measurements were performed. Nevertheless, some comments about adsorption properties of the composites can be given here. Graphite and aluminum are hydrophobic and non porous additives. These properties of the additives probably would affect the adsorption properties of the composites. In addition, decrease in the clinoptilolite content in the composites could decrease the adsorption capacity of the composites. On the other hand, aluminum hydroxide is porous and has ability to adsorb. Therefore, the composites containing aluminum hydroxide would have the highest adsorption capacity among all composites. The composites containing aluminum would have the lowest adsorption capacity since it was not porous.

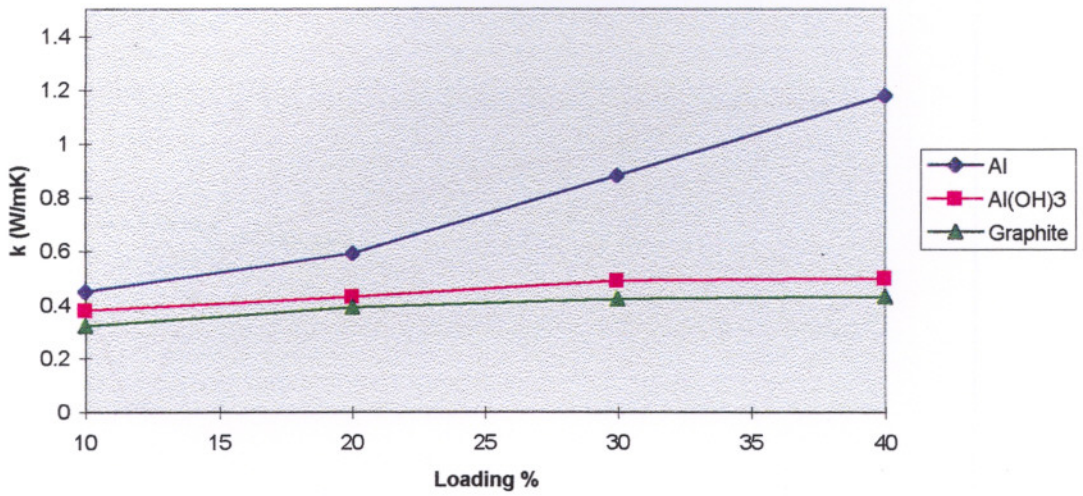


Figure 14 Densities of the composites versus composite loading

Density (bulk density) is another parameter for characterization. Thickness, diameter and mass of the pellets were measured to calculate the bulk densities. Since there were two samples for each composite an average of these values were taken. The variation of densities and the composite loading percentage is shown in Figure 14.

FAKULTAS TEKNIK
 KUTUBUNDA
 UNIVERSITAS SEBELAS MARET
 SURABAYA

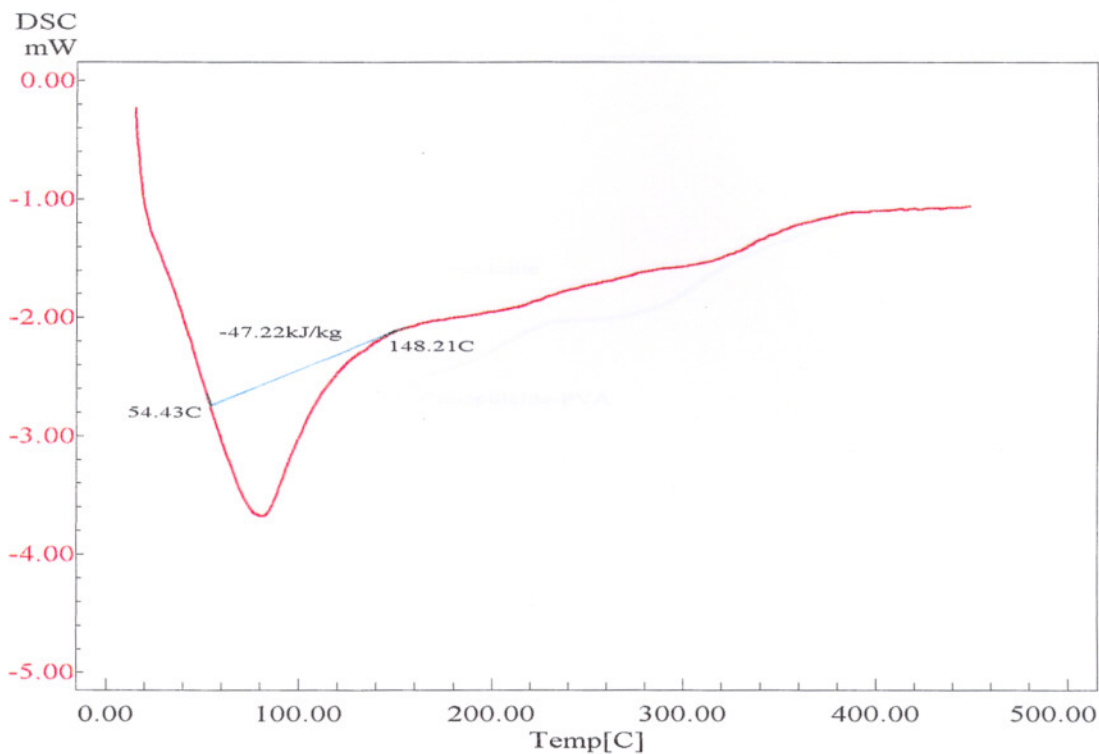


Figure 15 DSC analysis of the clinoptilolite

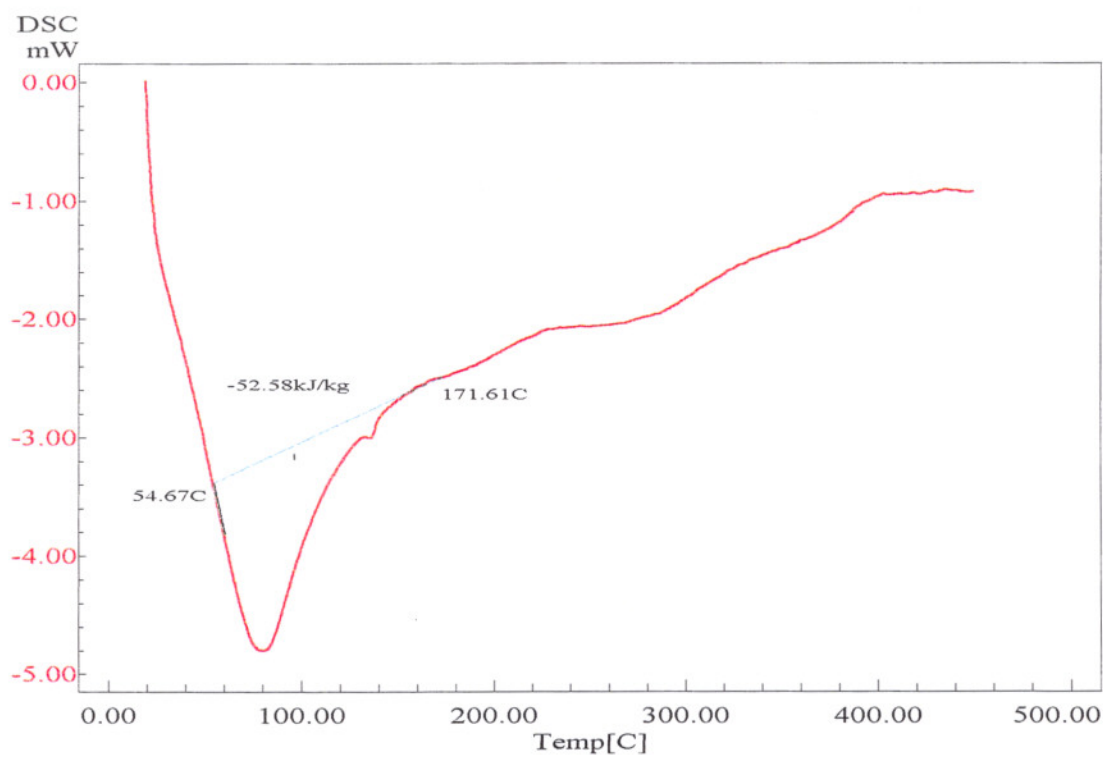


Figure 16 DSC analysis of the clinoptilolite containing polyvinylalcohol

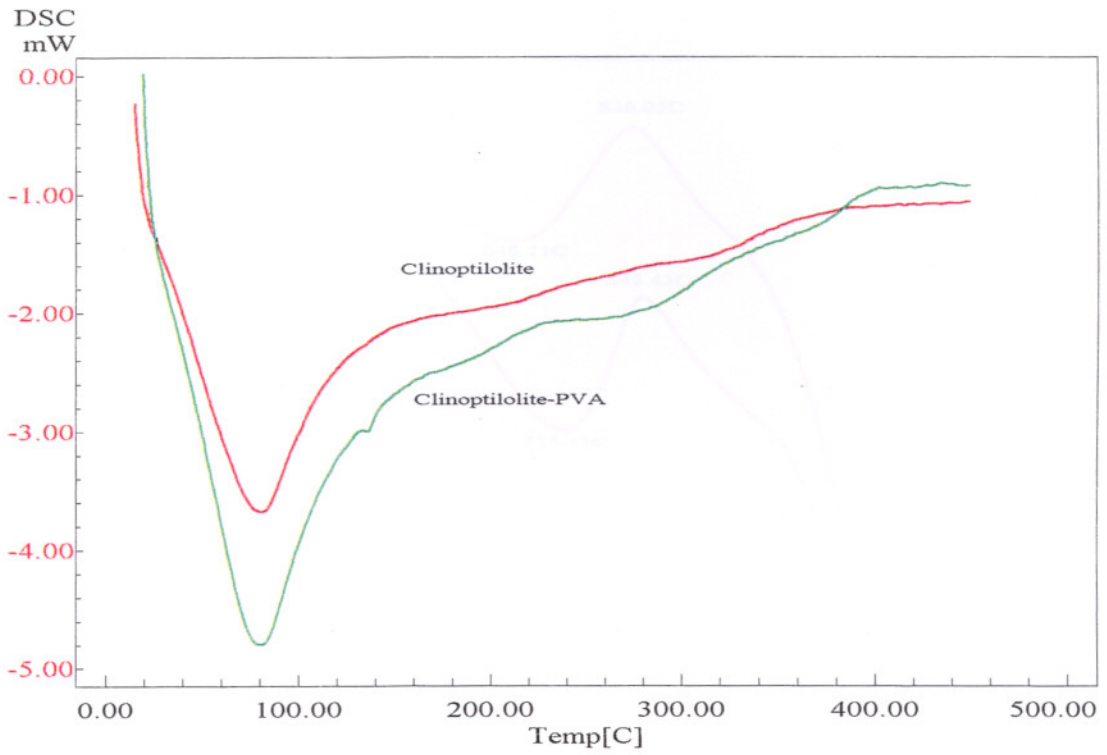


Figure 17 DSC analysis of the clinoptilolite and the clinoptilolite containing PVA

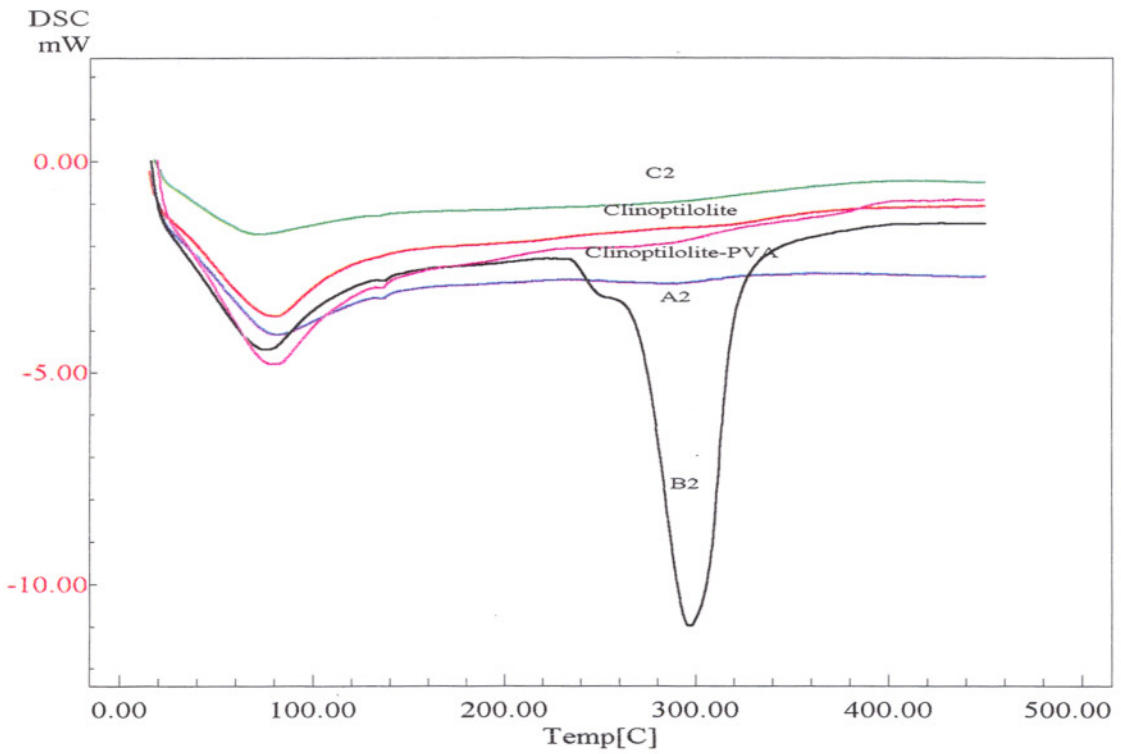


Figure 18 DSC analysis of the clinoptilolite, the clinoptilolite-PVA and the all composites containing %20 additive

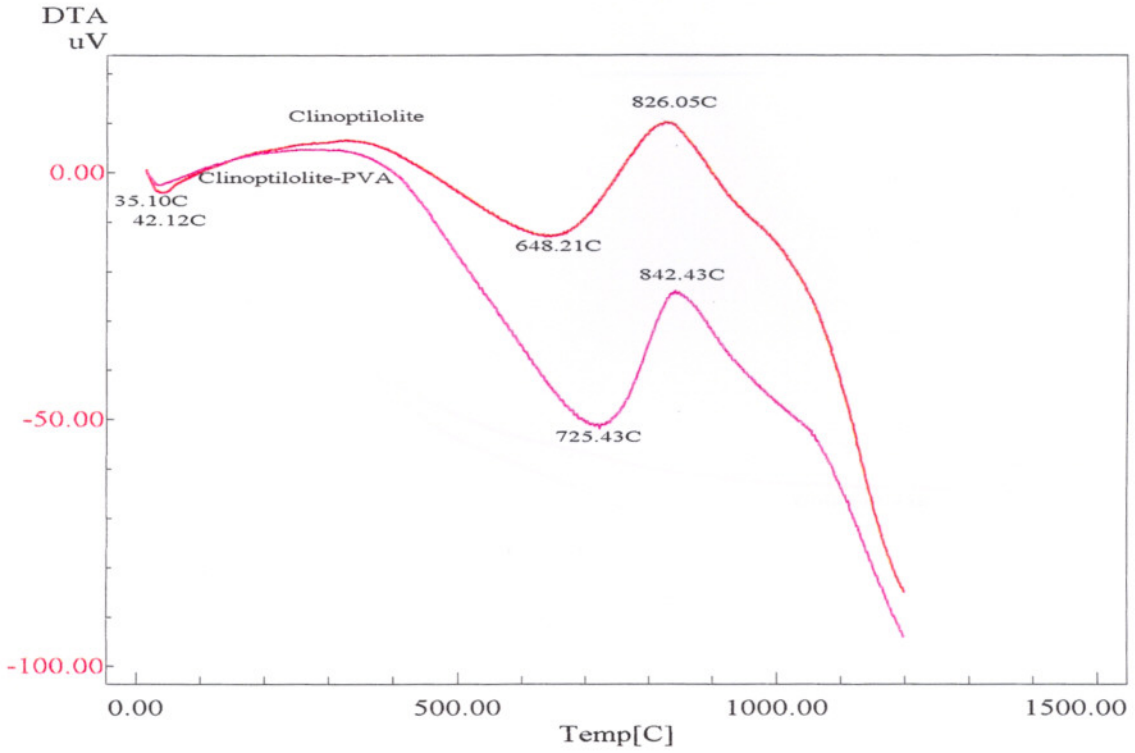


Figure 19 DTA analysis of the clinoptilolite and clinoptilolite containing PVA

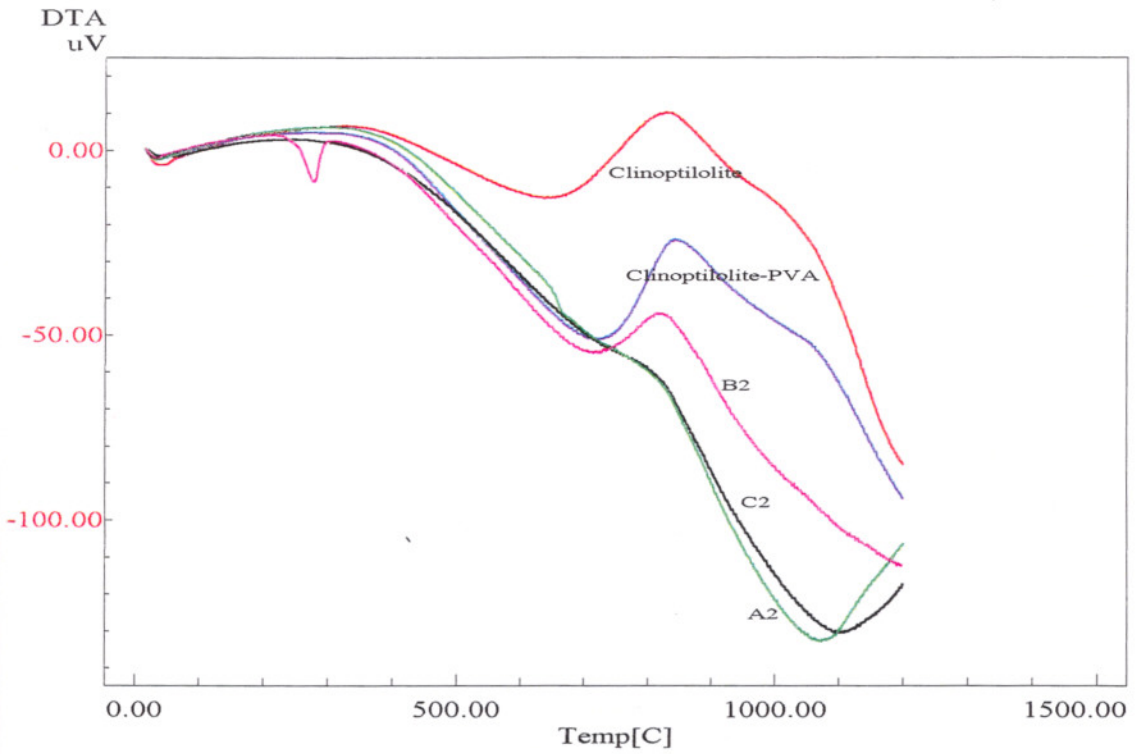


Figure 20 DTA analysis of the clinoptilolite, the clinoptilolite-PVA and all the composites containing 20% additive

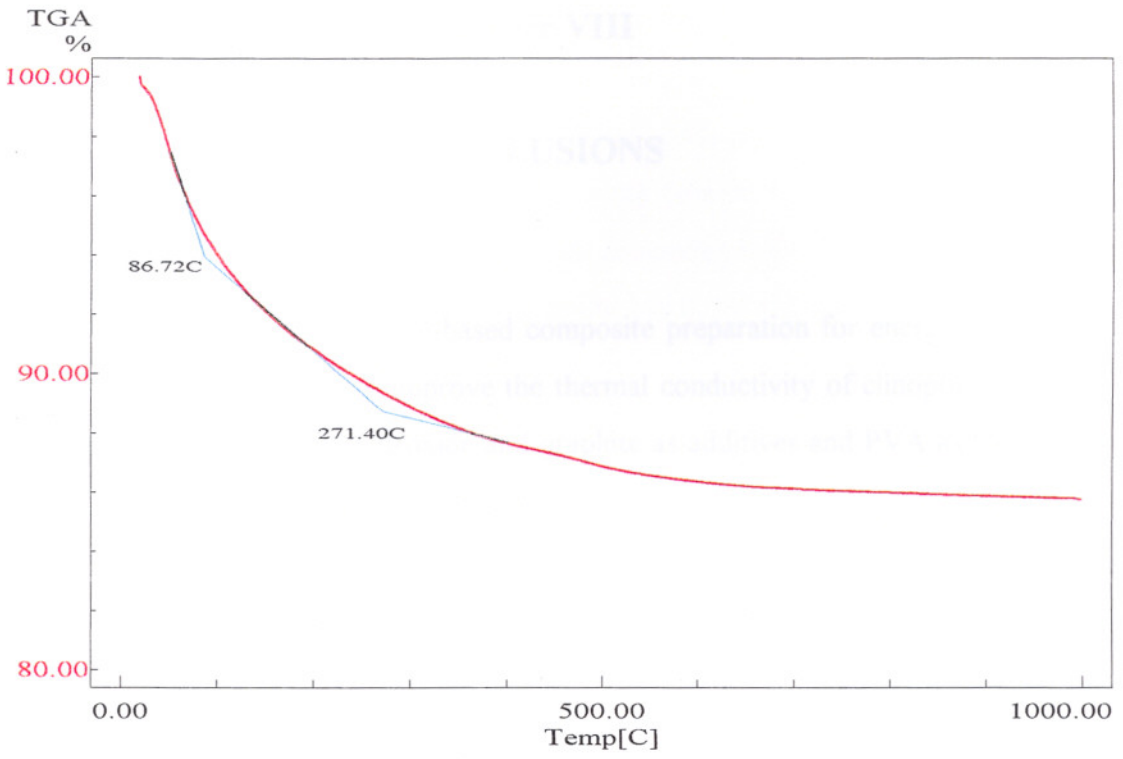


Figure 23 TGA analysis of the clinoptilolite

İZMİR YATIRIM TEKNOLOJİLERİ ANA BİRLİĞİ
İZMİR YATIRIM TEKNOLOJİLERİ ANA BİRLİĞİ
İZMİR YATIRIM TEKNOLOJİLERİ ANA BİRLİĞİ

Chapter VIII

CONCLUSIONS

In this work, clinoptilolite-based composite preparation for energy storage was investigated. Aim was to improve the thermal conductivity of clinoptilolite by using aluminum, aluminum hydroxide and graphite as additives and PVA as binder. The following conclusions could be drawn:

1. For composite preparation, powder route method was chosen to control composite preparation temperature and pressure.
2. An optimum thermal treatment temperature of 150 °C and press pressure of 60 bar were found for composite preparation.
3. Binder was needed to prepare intact composite pellets. For this purpose PVA was used.
4. The heat of dehydration for the clinoptilolite was determined as 47.22 kJ/kg. It changed differently for the additives. It was higher with composites containing aluminum hydroxide while it was lower for other additives.
5. Aluminum hydroxide started decomposing around 200 °C.
6. Clinoptilolite was unstable above 800 °C. PVA started decomposing at 230 °C. The composites containing graphite were destroyed at 630 °C.
7. TGA analysis of the sample showed that there exists about 14.22 % water in all the samples characterized.
8. There existed three types of water: external water, loosely bound water and tightly bound water in the clinoptilolite. Results obtained with DSC, DTA and TGA were consistent and in agreement with each other.
9. Thermal conductivities of the composites were high for additives having higher thermal conductivities. Composites containing 40% aluminium had the highest thermal conductivity value, 1.18 W/mK as it had the highest

thermal conductivity among all the additives and it had a very fine particle size distribution.

10. Addition of graphite increased thermal conductivity slightly. It increased from 0.32 to 0.43 by changing graphite content from 10 to 40 %. This might be due to the formation of an interconnected graphite network which favors heat transfer as graphite has a thermal conductivity of 5.70 W/mK (ref).
11. A little increase was observed in thermal conductivity of the composites containing aluminum hydroxide with respect to the composites containing graphite. By increasing loading from 10 to 40 %, thermal conductivity increased from 0.38 to 0.50 W/mK.
12. Adsorption properties of the composites were also important for energy storage applications. Therefore, adsorption capacity of the composites had to be investigated but there was no available data for this. Examinations of nature of additives and thermal analysis results suggested the composites containing aluminum hydroxide had the highest adsorption capacity among all composites prepared.

REFERENCES

- [1] B.Kılış and S.Kakaç, "Importance of Energy Storage", in *NATO ASI on Energy Storage Systems*, edited by S.Kakaç and B.Kılış, (Kluwer, Dordrecht,1989) p. 1
- [2] S.Kakaç, E.Paykoç and Y.Yener, "Storage of Solar Thermal Energy", in *NATO ASI on Energy Storage Systems*, edited by S.Kakaç and B.Kılış, (Kluwer, Dordrecht,1989) p. 129.
- [3] M.Suzuki, *Adsorption Engineering*, (Elsevier, Amsterdam, 1990), p. 1.
- [4] D.M.Ruthven, *Principles of Adsorption and Adsorption Processes*, (John Wiley, New York, 1984), p. 1.
- [5] S.Ülkü and M.Mobedi, "Adsorption in Energy Storage", in *NATO ASI on Energy Storage Systems*, edited by S.Kakaç and B.Kılış, (Kluwer, Dordrecht,1989) p. 487
- [6] A.Dyer, "What is a Zeolite", in *An Introduction to Zeolite Molecular Sieves*, (John Wiley and Sons,New York), p. 1.
- [7] D.W.Breck, *Zeolite Molecular Sieves*, (John Wiley and Sons, New York, 1974), p. 3.
- [8] F.A.Mumpton, *Natural Zeolites, Occurences, Properties, Use*, (Pergamon Press, 1978), p. 3.
- [9] H. van Koningsveld, "Structural Subunits in Silicate and Phosphate Structures", in *Introduction to Zeolite Science and Practice*, edited by H. van Bekkum, E.M.Flanigen and J.C.Jansen, (Elsevier, Amsterdam, 1991), p. 36.
- [10] S.Ülkü, "Novel Application of Adsorption: Energy Recovery", *Proceedings of the Fourth International Conference on Fundamentals of Adsorption* , edited by M.Suzuki, (Kodansha, 1992), p. 685.
- [11] S.Ülkü and M.Mobedi, "Zeolites in Heat Recovery", in *Zeolites:Facts, Figures, Future*, edited by P.A.Jacobs and R.A. van Santen, (Elsevier Science Publishers BV., Amsterdam, 1989) p. 511.
- [12] S.Ülkü, "Natural Zeolites in Energy Storage and Heat Pumps", *Proceedings of the 7th International Zeolite Conference*, (Tokyo, 1986), 1047

- [13] S.Ülkü, S.Beba, Z.Kıvrak and B.Seyrek, “Enerji Depolama ve Hava Kurutmada Doğal Zeolitlerden Yaralanma”, *Isı Bilimi ve Tekniği 5. Ulusal Kongresi*, (İstanbul, 1985), 549
- [14] S.Ülkü, “Adsorption Heat Pumps”, *Proceedings of the Symposium: Solid Sorption Refrigeration*, (Paris, 1992), 86
- [15] S.Ülkü, “Solar Adsorption Heat Pumps”, in *NATO ASI Solar Energy Utilization*, edited by M.Nijhoff, (Netherland, 1987), p. 424.
- [16] S.Ülkü, “Air Drying in Packed Bed Adsorbers”, in *Drying '86*, edited by J.J.Mujumdar, (Hemisphere, Washington, 1987), p. 807.
- [17] G.Alefeld, P.Maier and M.Rothmeyer, “Zeolite Heat Pump and Heat Transformer for Load Management”, *Proceedings of 16th International Society Energy Conversion Conference*, (New York, 1981), 855
- [18] D.I.Tchernev, “Regenerative Zeolite Heat Pump” in *Zeolites: Facts, Figures, Future*, edited by P.A.Jacobs and R.A. van Santen, (Elsevier Science Publishers BV., Amsterdam, 1989), p. 519.
- [19] D.Tchernev and D.Emerson “Closed Cycle Zeolite Regenerative Heat Pump” in *Zeolites: Facts, Figures, Future*, edited by P.A.Jacobs and R.A. van Santen, (Elsevier Science Publishers BV., Amsterdam, 1989), p. 747.
- [20] G.Restuccia, G.Cacciola and R.Quagliata, “Identification of Zeolites for Heat Transformer, Chemical Heat Pump and Cooling Systems”, *International Journal of Energy Research*, 12 (1988), 101
- [21] G.Gottardi and E.Galli, *Natural Zeolites*, (Springer-Verlag, Berlin, 1985), p. 1.
- [22] Z.Y.Liu, G.Cacciola, G.Restuccia, and N.Giordano, “Fast, Simple and Accurate Measurement of Zeolite Thermal Conductivity”, *Zeolites*, 10 (1990), 565
- [23] L.Pino, Y.Aristov, G.Cacciola, and G.Restuccia, “Composite Materials Based on Zeolite 4A for Adsorption Heat Pumps”, *Adsorption*, 3 (1996), 33
- [24] M.Groll, “Reaction Beds for Dry Sorption Machines”, *Proceedings of the Symposium: Solid Sorption Refrigeration*, (Paris, 1992), 207

- [25] J.J.Guilleminot and J.M. Gurgel, "Heat Transfer Intensification in Adsorbent Beds of Adsorption Thermal Devices", in *The Twelfth Annual ASME International Solar Energy Conference*, edited by ASME, (New York, 1990), p. 69.
- [26] J.J.Guilleminot, A.Choisier, J.B.Chalfen, S.Nicholas, and J.L.Reymonet, "Amelioration Des Transfers Thermiques Dans Les Adsorbours a Lits Fixes Consolides", *Proceedings of the Symposium: Solid Sorption Refrigeration*, (Paris, 1992), 200
- [27] H.Sahnoune and PH.Grenier, "Mesure de la Conductivite Thermique d'une Zeolithe", *The Chemical Engineering Journal*, 40 (1989), 45
- [28] D.I.Tchernev and D.T.Emerson, *Ashrae Trans.* , part 2 (1988), 94
- [29] J.Volkl, *7th International Heat Transfer Conference*, 2 (1982), 105
- [30] F.L.Slejko, *Adsorption Technology* , (Marcel Dekker, New York, 1985), p. 1.
- [31] M.Suziki, *Adsorption Engineering* , (Elsevier, Amsterdam, 1990), p. 1.
- [32] A.F.Cronstedt, *Akad. Handl.*, 18 (Stockholm,1756), 120
- [33] A.Damour, *Ann. Mines*, 17 (1840), 191
- [34] H.Eichorn, *Poggendorf Ann. Phys. Chem.*, 105 (1858), 126
- [35] O.Weigel and E.Steinhoff, *Z. Kristallogr.*, 61 (1925), 125
- [36] Mc.Bain, *The Sorption of Gases and Vapors by Solid* , (Rutledge and Sons, London, 1932), p. 1.
- [37] Holometrix Company Instruction Manuel
- [38] Guarded Heat Flow Meter Method- ASTM F433
- [39] Heat Flow Meter Method- ASTM C518
- [40] Guarded Hot Plate Method- ASTM C177
- [41] K.K.Chawla, *Composite Materials* , (Springer-Verlag, 1988), p. 1.
- [42] J.S.Reed, "Communion", in *Principles of Ceramics Processing*, (John Wiley and Sons, New York, 1995), p. 313.
- [43] F.P.Incropera and D.P.De Witt, *Fundamentals of Heat and Mass Transfer*, (John Wiley and Sons, New York, 1990), A1.

APPENDIX A

A.1. MATERIAL PROPERTIES

Table 13 Properties of Aluminium

Assay (by complexometry)	> 90%
Heavy metals (as Pb)	< 0.03%
As (Arsenic)	< 0.0005%
Fe (iron)	< 0.5%
Fats	< 1%
Molecular Weight, g/Mol	26.98

Table 14 Properties of Aluminium hydroxide

Chemical formula	Al(OH)_3
Molecular Weight, g/Mol	78

Table 15 Properties of PVA

Property	Polyvinyl alcohol (PVA)
Chemical structure	$[-\text{CH}_2\text{CH(OH)}-]_x-$ $[-\text{CH}_2\text{CHCO}_2\text{CCH}_3-]_y$
Average Molecular Weight, g/Mol	9000-1000
Percentage of hydrolization	80%

Table 16 Properties of graphite

Type	Synthetic
Particle size	1-2 μm

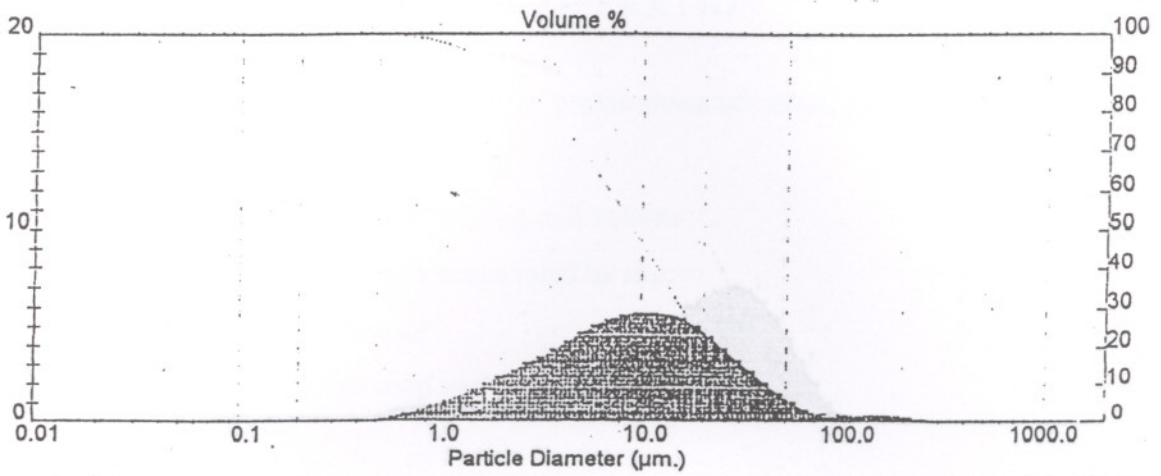


Table 10 Particle size analysis of the clinoptilolite

System Details			
Range Lens: 300 mm	Beam Length: 2.40 mm	Sampler: MS17	Obscuration: 8.5 %
Presentation: 3OHD	[Particle R.I. = (1.5295, 0.1000):	Dispersant R.I. = 1.3300]	Residual: 0.324 %
Analysis Model: Polydisperse			
Modifications: None			

Result Statistics			
Distribution Type: Volume	Concentration = 0.0059 %Vol	Density = 1.000 g / cub. cm	Specific S.A. = 1.1792 sq. m / g
Mean Diameters:	D (v, 0.1) = 2.12 µm	D (v, 0.5) = 9.12 µm	D (v, 0.9) = 32.74 µm
D [4, 3] = 15.91 µm	D [3, 2] = 5.09 µm	Span = 3.313E+00	Uniformity = 1.254E+00

Size Low (µm)	In %	Size High (µm)	Under%	Size Low (µm)	In %	Size High (µm)	Under%
0.49	0.12	0.58	0.12	22.49	3.96	26.20	85.57
0.58	0.26	0.67	0.39	26.20	3.33	30.53	88.91
0.67	0.42	0.78	0.81	30.53	2.71	35.56	91.62
0.78	0.65	0.91	1.46	35.56	2.12	41.43	93.73
0.91	0.89	1.06	2.35	41.43	1.59	48.27	95.32
1.06	1.15	1.24	3.50	48.27	1.12	56.23	96.44
1.24	1.44	1.44	4.94	56.23	0.73	65.51	97.17
1.44	1.74	1.68	6.68	65.51	0.43	76.32	97.60
1.68	2.07	1.95	8.75	76.32	0.24	88.91	97.84
1.95	2.41	2.28	11.16	88.91	0.37	103.58	98.21
2.28	2.76	2.65	13.92	103.58	0.32	120.67	98.53
2.65	3.12	3.09	17.03	120.67	0.36	140.58	98.80
3.09	3.49	3.60	20.52	140.58	0.38	163.77	99.28
3.60	3.89	4.19	24.42	163.77	0.33	190.80	99.61
4.19	4.31	4.88	28.73	190.80	0.23	222.28	99.84
4.88	4.72	5.69	33.44	222.28	0.12	258.95	99.96
5.69	5.08	6.63	38.53	258.95	0.04	301.68	100.00
6.63	5.38	7.72	43.90	301.68	0.00	351.46	100.00
7.72	5.59	9.00	49.49	351.46	0.00	409.45	100.00
9.00	5.70	10.48	55.19	409.45	0.00	477.01	100.00
10.48	5.70	12.21	60.89	477.01	0.00	555.71	100.00
12.21	5.62	14.22	66.51	555.71	0.00	647.41	100.00
14.22	5.48	16.57	71.99	647.41	0.00	754.23	100.00
16.57	5.07	19.31	77.06	754.23	0.00	878.67	100.00
19.31	4.55	22.49	81.61				

Figure 24 Particle size distribution of the clinoptilolite

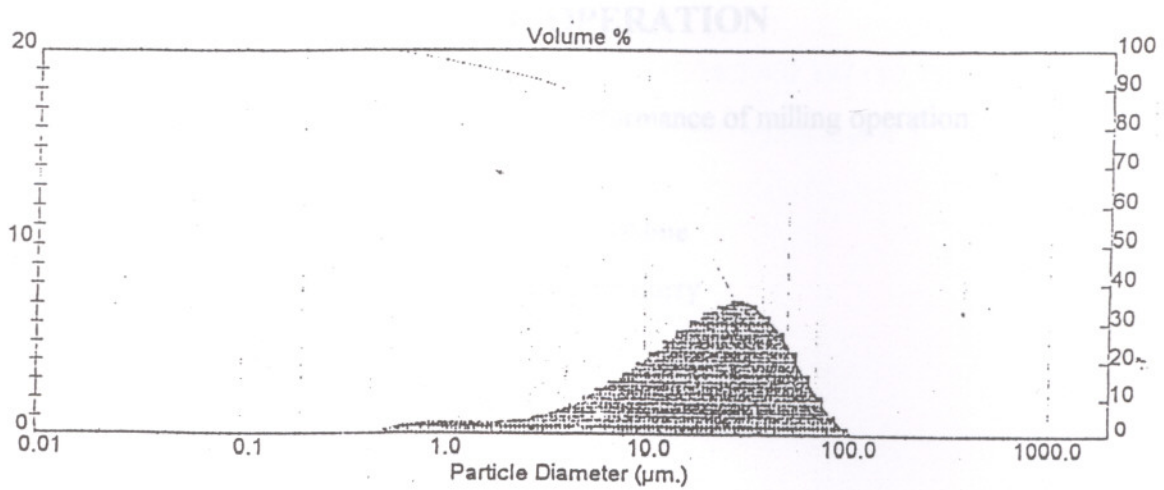


Table 11 Particle size analysis of the aluminum hydroxide

System Details			
Range Lens: 300 mm	Beam Length: 2.40 mm	Sampler: MS17	Obscuration: 12.0 %
Presentation: 30HD	(Particle R.I. = (1.5295, 0.1000);	Dispersant R.I. = 1.3300]	Residual: 0.312 %
Analysis Model: Polydisperse			
Modifications: None			

Result Statistics			
Distribution Type: Volume	Concentration = 0.0140 %Vol	Density = 1.000 g / cub. cm	Specific S.A. = 0.7713 sq. m / g
Mean Diameters:	D (v, 0.1) = 3.86 µm	D (v, 0.5) = 19.93 µm	D (v, 0.9) = 50.82 µm
D [4, 3] = 24.26 µm	D [3, 2] = 7.78 µm	Span = 2.357E+00	Uniformity = 7.312E-01

Size Low (µm)	In %	Size High (µm)	Under%	Size Low (µm)	In %	Size High (µm)	Under%
0.49	0.24	0.58	0.24	22.49	6.93	26.20	62.18
0.58	0.46	0.67	0.70	26.20	7.20	30.53	69.38
0.67	0.63	0.78	1.32	30.53	6.97	35.56	76.35
0.78	0.68	0.91	2.01	35.56	6.43	41.43	82.78
0.91	0.73	1.06	2.73	41.43	5.58	48.27	88.35
1.06	0.74	1.24	3.47	48.27	4.49	56.23	92.85
1.24	0.73	1.44	4.21	56.23	3.30	65.51	96.15
1.44	0.72	1.68	4.93	65.51	2.16	76.32	98.31
1.68	0.72	1.95	5.65	76.32	1.20	88.91	99.51
1.95	0.75	2.28	6.40	88.91	0.49	103.58	100.00
2.28	0.83	2.65	7.23	103.58	0.00	120.67	100.00
2.65	0.98	3.09	8.21	120.67	0.00	140.58	100.00
3.09	1.18	3.60	9.38	140.58	0.00	163.77	100.00
3.60	1.42	4.19	10.81	163.77	0.00	190.80	100.00
4.19	1.73	4.88	12.53	190.80	0.00	222.28	100.00
4.88	2.08	5.69	14.62	222.28	0.00	258.95	100.00
5.69	2.48	6.63	17.10	258.95	0.00	301.68	100.00
6.63	2.91	7.72	20.01	301.68	0.00	351.46	100.00
7.72	3.39	9.00	23.40	351.46	0.00	409.45	100.00
9.00	3.92	10.48	27.32	409.45	0.00	477.01	100.00
10.48	4.48	12.21	31.80	477.01	0.00	555.71	100.00
12.21	5.07	14.22	36.87	555.71	0.00	647.41	100.00
14.22	5.64	16.57	42.50	647.41	0.00	754.23	100.00
16.57	6.16	19.31	48.66	754.23	0.00	878.67	100.00
19.31	6.59	22.49	55.25				

Figure 25 Particle size distribution of the aluminum hydroxide



A.2. MILLING OPERATION

There are some factors affecting the performance of milling operation:

1. The percentage of media filling mill volume
2. The percentage of void space filled by slurry
3. Critical speed of the jar
4. The percentage of solid in slurry

Since it is an easy way to obtain fine powders, wet milling was preferred and ethanol was used as a liquid and zirconia balls as a grinding media.

In ball-milling, diameter of the container, D , is 0.3215 feet and radius of the container, R , was 0.049 meter. The ideal rotation speed, w_{cr} , is one of the main parameters in milling and can be determined from the equation [42]:

$$w_{cr} = 1 / 2R^{-1/2}$$

$$w_{cr} = 1 / 2R^{-1/2} = 2.26 \text{ sec}^{-1} \quad \text{and} \quad w_c = 2.26 * 60 = 135 \text{ rpm}$$

Ideal rotation speed lies between $0.65 w_c - 0.85 w_c$ and assuming $0.75 w_c$, and

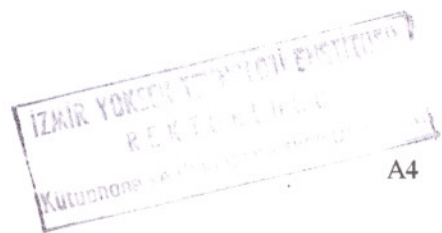
$75 * 135 = 101 \text{ rpm}$ is the rotation speed in this case.

For zirconia balls, the bulk volume, (V_{bulk}), and the void volume, (V_{void}) are 220.4 cm^3 and 554.7 cm^3 respectively. Mill volume (volume of the container) is 1260 cm^3 . 5% of the bulk volume was exceeded to prepare natural zeolite and ethanol for wet milling.

Then, the total volume of natural zeolite and ethanol occupied in the container can be found as $1.05 * 220.4 = 231.4 \text{ cc}$

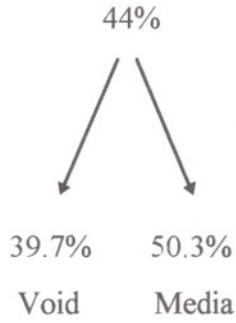
For 75 cc portion of this volume: there were 50 g zeolite and 61.5 cc ethanol = 75 cc (over 96.4 gr of total mass). Now density of the slurry can be calculated as

$$\rho_{slurry} = 96.4 / 75 = 1.285 \text{ g / cm}^3$$



Percentage of the volume of the void space, $220.4 / 554.7 = 0.397$ (39.7%)

Percentage of the bulk volume, $554.7 / 1260 = 0.44$ (44%)



After 4 hour milling, the slurry was dried at 65°C and separated in terms of particle size using molecular sieves. Finally, clinoptilolite particles with diameters less than $45\ \mu\text{m}$ were obtained and they were used for composite preparation.

IZMIR YÜKSEK TEKNİK ENSTİTÜSÜ
KUTUPHANESİ

A.4. THERMOCOUPLE CALIBRATION

Thermocouples were calibrated by using constant temperature water bath. Temperature readings for five thermocouples (x values) were taken and at the same time, thermometer readings (y values) were read (Table 12).

Table 12 Calibration data for thermocouple

X ₄	Y ₄	X ₅	Y ₅	X ₆	Y ₆	X ₇	Y ₇	X ₈	Y ₈
49.46	52.15	49.49	52.15	49.47	52.15	49.49	52.15	49.51	52.15
53.43	56.10	53.45	56.10	53.47	56.10	53.47	56.10	53.47	56.10
57.55	60.00	57.59	60.00	57.53	60.00	57.59	60.00	57.62	60.00
61.58	63.95	61.58	63.95	61.54	63.95	61.60	63.95	61.60	63.95
65.69	67.95	65.69	67.95	65.67	67.95	65.71	67.95	65.75	67.95
69.76	71.90	69.74	71.90	69.76	71.90	69.76	71.90	69.80	71.90
73.80	75.90	73.81	75.90	73.75	75.90	73.79	75.90	73.87	75.90
77.80	79.90	77.84	79.90	77.82	79.90	77.84	79.90	77.88	79.90
81.79	83.85	81.83	83.85	81.79	83.85	81.81	83.85	81.85	83.85
85.86	87.80	85.88	87.80	85.86	87.80	85.92	87.80	85.96	87.80
89.81	91.80	89.91	91.80	89.89	91.80	89.89	91.80	89.89	91.80
93.88	95.75	93.88	95.75	93.86	95.75	93.90	95.75	93.92	95.75

Channel 4

Expression: $y = c_1 + c_2 * x$

Sum of squares: 0.0586257273608719

Standard error: 0.0698961893100952

Completed 7 iterations (Marquardt)

$c_1 = 3.51053185992164$

$c_2 = 0.982001159540772$

X-range: from 0 to 93.88

Y-range: from 0 to 95.75

X mean: 66.1853846153846;

standard deviation: 23.3375506642389

Y mean: 68.2346153846154;

standard deviation: 23.6895253111466

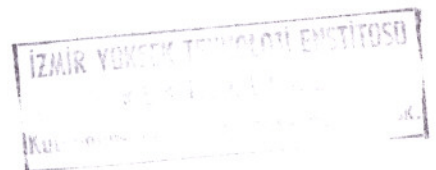
13 data points

Channel 5

Expression: $y = c_1 + c_2 * x$

Sum of squares: 0.0395533312961187

Standard error: 0.0574117665757049



Completed 7 iterations (Marquardt)

$$c_1 = 3.52373362152968$$

$$c_2 = 0.981497631599814$$

X-range: from 0 to 93.88

Y-range: from 0 to 95.75

X mean: 66.2069230769231;

standard deviation: 23.3466216909149

Y mean: 68.2346153846154;

standard deviation: 23.6895253111466

13 data points

Channel 6

Expression: $y = c_1 + c_2 \cdot x$

Sum of squares: 0.0337444617008805

Standard error: 0.0530286571117295

Completed 7 iterations (Marquardt)

$$c_1 = 3.53678362624053$$

$$c_2 = 0.981635030375428$$

X-range: from 0 to 93.86

Y-range: from 0 to 95.75

X mean: 66.1853846153846;

standard deviation: 23.3404639118699

Y mean: 68.2346153846154;

standard deviation: 23.6895253111466

13 data points

Channel 7

Expression: $y = c_1 + c_2 \cdot x$

Sum of squares: 0.0412301225268962

Standard error: 0.0586160689905764

Completed 7 iterations (Marquardt)

$$c_1 = 3.50743053229222$$

$$c_2 = 0.98163369263856$$

X-range: from 0 to 93.9

Y-range: from 0 to 95.75

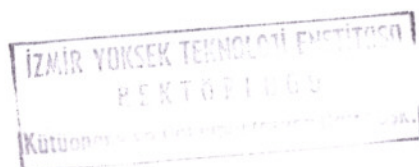
X mean: 66.2130769230769;

standard deviation: 23.3470058645694

Y mean: 68.2346153846154;

standard deviation: 23.6895253111466

13 data points



Channel 8

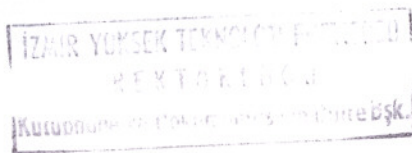
Expression: $y = c_1 + c_2 * x$
 Sum of squares: 0.0646902436850357
 Standard error: 0.0734224328146354
 Completed 9 iterations (Marquardt)

$c_1 = 3.49837642877962$
 $c_2 = 0.981360882170779$

X-range: from 0 to 93.92
 Y-range: from 0 to 95.75
 X mean: 66.24;
 standard deviation: 23.3554688044775
 Y mean: 68.2346153846154;
 standard deviation: 23.6895253111466
 13 data points

To correct all readings of the thermocouples, a linear relationship was obtained as an expression $y = c_1 + c_2 * x$ and after finding the constants c_1 and c_2 , the equations were driven by using calibration data in Table 13. Marquart method is used in order to find the constants in the calibration equations. Then, thermocouple readings can be corrected by the equations given below:

- T_4 (corrected) = $0.982001159540772T_4 + 3.51053185992164$
- T_5 (corrected) = $0.981497631599814T_5 + 3.52373362152968$
- T_6 (corrected) = $0.981635030375428T_6 + 3.53678362624053$
- T_7 (corrected) = $0.98163369263856T_7 + 3.50743053229222$
- T_8 (corrected) = $0.981360882170779T_5 + 3.49837642877962$



A.5. THERMOCONDUCTIVITY DATA AND FIGURES

Table 17 Thermal conductivity data of the clinoptilolite

Time	T _{ambient}	T ₄	T ₅	T ₇	T ₈	k ₁	k ₂
1	18.33	27.11	42.12	41.51	27.61	0.04	0.05
10	19.17	35.20	57.03	56.01	36.51	0.03	0.03
20	19.49	41.63	50.02	49.72	42.55	0.08	0.10
30	19.37	42.88	47.18	47.05	43.45	0.16	0.20
40	19.24	42.89	46.16	46.09	43.21	0.22	0.25
50	19.16	42.63	45.61	45.54	42.89	0.24	0.27
60	19.11	42.46	45.25	45.24	42.55	0.26	0.27
70	19.08	42.13	44.92	44.79	42.22	0.26	0.28
80	19.08	41.76	44.57	44.50	41.86	0.26	0.27
90	19.05	41.56	44.18	44.17	41.56	0.27	0.27
100	19.03	41.23	43.86	43.79	41.17	0.27	0.27
110	19.03	41.00	43.62	43.48	40.92	0.27	0.28
120	19.02	40.67	43.31	43.30	40.68	0.27	0.27
130	19.01	40.49	43.12	43.05	40.44	0.27	0.27
140	19	40.19	42.88	42.87	40.19	0.27	0.27
150	18.98	40.06	42.68	42.60	39.99	0.27	0.27
160	18.98	39.76	42.45	42.38	39.75	0.27	0.27
170	18.96	39.62	42.24	42.23	39.62	0.27	0.27
180	18.97	39.44	42.13	42.06	39.46	0.27	0.27
190	18.96	39.39	42.01	41.94	39.33	0.27	0.27
200	18.96	39.14	41.83	41.76	39.15	0.27	0.27
210	18.94	39.00	41.69	41.61	39.02	0.27	0.28
220	18.93	38.94	41.56	41.43	38.88	0.27	0.28
230	18.92	38.80	41.48	41.35	38.81	0.27	0.28
240	18.92	38.68	41.37	41.23	38.69	0.27	0.28
250	18.91	38.61	41.23	41.11	38.56	0.27	0.28
260	18.93	38.50	41.13	41.00	38.45	0.27	0.28
270	18.92	38.38	41.00	40.93	38.34	0.27	0.28
280	18.9	38.31	40.98	40.85	38.26	0.27	0.28
290	18.9	38.18	40.87	40.84	38.24	0.27	0.28
300	18.91	38.13	40.82	40.69	38.14	0.27	0.28
310	18.89	38.11	40.75	40.61	38.08	0.27	0.28
320	18.89	38.05	40.68	40.61	38.02	0.27	0.28
330	18.88	38.04	40.64	40.59	38.00	0.28	0.28
340	18.87	37.98	40.60	40.55	37.94	0.26	0.26
350	18.87	37.92	40.54	40.55	37.94	0.26	0.26
360	18.87	37.89	40.51	40.35	37.73	0.26	0.26
370	18.88	37.87	40.50	40.42	37.79	0.26	0.26
380	18.86	37.80	40.43	40.27	37.64	0.26	0.26
390	18.87	37.74	40.36	40.29	37.67	0.26	0.26

Table 18 Thermal conductivity data of the clinoptilolite containing PVA

Time	T _{ambient}	T ₄	T ₅	T ₇	T ₈	k ₁	k ₂
1	18.33	27.11	42.12	41.51	27.28	0.05	0.05
10	19.17	35.20	57.03	56.01	36.28	0.03	0.03
20	19.49	41.63	50.02	49.72	42.38	0.09	0.10
30	19.37	42.88	47.18	47.05	43.29	0.18	0.20
40	19.24	42.89	46.16	46.09	43.05	0.24	0.25
50	19.16	42.63	45.61	45.54	42.73	0.26	0.27
60	19.11	42.46	45.25	45.24	42.38	0.28	0.27
70	19.08	42.13	44.92	44.79	42.05	0.28	0.28
80	19.08	41.76	44.57	44.50	41.69	0.28	0.27
90	19.05	41.44	44.18	44.17	41.29	0.28	0.27
100	19.03	41.12	43.86	43.79	40.99	0.28	0.28
110	19.03	40.88	43.62	43.48	40.74	0.28	0.28
120	19.02	40.63	43.31	43.30	40.49	0.29	0.27
130	19.01	40.38	43.12	43.05	40.24	0.28	0.27
140	19.00	40.19	42.88	42.87	40.00	0.29	0.27
150	18.98	39.94	42.68	42.60	39.79	0.28	0.27
160	18.98	39.76	42.44	42.38	39.63	0.29	0.28
170	18.96	39.62	42.24	42.23	39.42	0.30	0.27
180	18.97	39.44	42.13	42.06	39.25	0.29	0.27
190	18.96	39.39	42.01	41.94	39.13	0.29	0.27
200	18.96	39.14	41.83	41.76	38.95	0.29	0.27
210	18.94	39.00	41.69	41.61	38.81	0.29	0.28
220	18.93	38.94	41.56	41.43	38.67	0.29	0.28
230	18.92	38.80	41.48	41.35	38.61	0.29	0.28
240	18.92	38.68	41.37	41.23	38.48	0.29	0.28
250	18.91	38.61	41.23	41.11	38.35	0.30	0.28
260	18.93	38.50	41.13	41.00	38.31	0.29	0.29
270	18.92	38.38	41.00	40.93	38.12	0.29	0.27
280	18.9	38.31	40.98	40.85	38.05	0.29	0.27
290	18.9	38.18	40.86	40.74	38.05	0.29	0.29
300	18.91	38.13	40.82	40.69	37.93	0.29	0.28
310	18.89	38.11	40.75	40.61	37.86	0.29	0.28
320	18.89	38.05	40.68	40.61	37.80	0.29	0.27
330	18.88	38.04	40.61	40.53	37.79	0.30	0.28
340	18.87	37.92	40.60	40.47	37.66	0.29	0.27
350	18.87	37.92	40.58	40.47	37.68	0.29	0.28
360	18.87	37.80	40.48	40.39	37.65	0.29	0.28
370	18.88	37.87	40.55	40.42	37.61	0.30	0.28
380	18.86	37.79	40.41	40.39	37.58	0.30	0.28
390	18.87	37.74	40.36	40.35	37.55	0.30	0.28
400	18.87	37.73	40.36	40.33	37.53	0.30	0.28
410	18.87	37.73	40.36	40.29	37.48	0.30	0.28

Table 19 Thermal conductivity data of the composite containing 10% aluminium

Time	T _{ambient}	T ₄	T ₅	T ₇	T ₈	k ₁	k ₂
1	19.71	23.38	23.42	23.36	23.29	23.13	16.33
10	19.64	30.81	44.34	44.81	30.41	0.08	0.08
20	19.59	42.81	52.56	52.98	41.45	0.12	0.10
30	19.57	45.42	48.63	48.26	44.30	0.37	0.30
40	19.54	45.62	48.35	47.75	44.87	0.44	0.41
50	19.53	45.61	48.14	47.79	45.09	0.47	0.44
60	19.48	45.56	48.02	47.69	45.16	0.49	0.47
70	19.45	45.59	48.00	47.77	45.26	0.50	0.47
80	19.41	45.60	48.02	47.79	45.27	0.49	0.47
90	19.41	45.61	48.08	47.91	45.34	0.48	0.46
100	19.43	45.56	48.03	47.81	45.23	0.48	0.46
110	19.44	45.52	47.97	47.81	45.30	0.49	0.47
120	19.44	45.57	47.99	47.81	45.30	0.49	0.47
130	19.46	45.54	47.98	47.83	45.31	0.49	0.47
140	19.46	45.59	48.07	47.97	45.39	0.48	0.46
150	19.47	45.55	48.04	47.84	45.32	0.48	0.47
160	19.46	45.55	48.06	47.90	45.37	0.48	0.47
170	19.44	45.57	48.09	47.94	45.36	0.47	0.46
180	19.41	45.60	48.07	47.97	45.45	0.48	0.47
190	19.38	45.64	48.09	48.01	45.42	0.49	0.46
200	19.36	45.61	48.06	48.05	45.47	0.49	0.46
210	19.34	45.67	48.18	48.09	45.56	0.48	0.47
220	19.31	45.69	48.22	48.17	45.59	0.47	0.46
230	19.27	45.77	48.35	48.25	45.61	0.46	0.45
240	19.21	45.77	48.33	48.26	45.67	0.47	0.46
250	19.17	45.79	48.34	48.33	45.75	0.47	0.46
260	19.12	45.87	48.39	48.42	45.78	0.47	0.45
270	19.08	45.88	48.35	48.42	45.84	0.48	0.46
280	19.03	45.90	48.44	48.50	45.86	0.47	0.45
290	18.99	45.93	48.45	48.52	45.89	0.47	0.45
300	18.96	46.01	48.47	48.62	46.04	0.48	0.46
310	18.92	45.98	48.48	48.58	45.99	0.48	0.46
320	18.89	46.05	48.56	48.68	46.03	0.47	0.45
330	18.85	46.03	48.56	48.64	45.99	0.47	0.45
340	18.83	46.07	48.58	48.67	46.03	0.47	0.45
350	18.79	46.09	48.59	48.64	46.06	0.48	0.46
360	18.77	46.09	48.62	48.67	46.03	0.46	0.44
370	18.75	46.09	48.61	48.83	46.19	0.46	0.44
380	18.72	46.09	48.63	48.80	46.15	0.46	0.44
390	18.7	46.09	48.61	48.78	46.13	0.46	0.44
400	18.67	46.11	48.65	48.76	46.10	0.46	0.44
410	18.65	46.13	48.66	48.78	46.12	0.46	0.44
420	18.61	46.15	48.68	48.77	46.12	0.46	0.44

Table 20 Thermal conductivity data of the composite containing 20% aluminium

Time	T _{ambient}	T ₄	T ₅	T ₇	T ₈	k ₁	k ₂
1	18.18	35.023	50.3608	48.093	32.1487	0.06589	0.06338
10	18.25	42.17	47.8678	46.012	38.8211	0.17736	0.14053
20	18.27	43.421	45.3944	44.245	40.9819	0.51215	0.30968
30	18.25	43.571	44.9527	44.098	41.9323	0.73157	0.46662
40	18.21	43.601	44.9233	44.245	42.3824	0.76449	0.5425
50	18.17	43.611	44.992	44.383	42.6425	0.73198	0.58075
60	18.12	43.631	45.0607	44.51	42.8926	0.70705	0.62472
70	18.08	43.571	45.1294	44.589	42.9626	0.64862	0.62145
80	18.03	43.651	45.2079	44.746	43.1127	0.64927	0.61878
90	17.97	43.812	45.365	44.815	43.2027	0.65057	0.62697
100	17.94	43.882	45.3748	44.893	43.3328	0.67683	0.64767
110	17.91	43.842	45.4533	45.05	43.3028	0.62704	0.57833
120	17.88	43.942	45.5613	45.188	43.4628	0.62399	0.58592
130	17.88	43.912	45.4631	45.099	43.4328	0.65139	0.60643
140	17.87	44.032	45.5809	45.109	43.5429	0.65238	0.64524
150	17.82	43.942	45.6104	45.207	43.4628	0.60564	0.57932
160	17.81	44.062	45.7281	45.276	43.5829	0.60649	0.59689
170	17.8	44.052	45.6594	45.207	43.5729	0.62864	0.61833
180	17.81	43.992	45.6104	45.148	43.5129	0.62437	0.61791
190	17.8	44.112	45.7183	45.266	43.6329	0.62909	0.61876
200	17.79	44.032	45.6496	45.188	43.5529	0.62467	0.61819
210	17.78	44.042	45.6889	45.266	43.6029	0.61358	0.60759
220	17.76	44.092	45.6987	45.246	43.6129	0.62894	0.61861
230	17.76	44.132	45.7968	45.335	43.6529	0.60699	0.60084
240	17.75	44.112	45.7183	45.266	43.6329	0.62909	0.61876
250	17.73	44.092	45.7085	45.256	43.6229	0.62512	0.61869
260	17.74	44.152	45.7576	45.256	43.6129	0.6294	0.61492
270	17.7	44.082	45.7478	45.354	43.6629	0.60663	0.59742
280	17.76	44.142	45.7478	45.305	43.6529	0.62932	0.61155
290	17.69	44.072	45.7674	45.374	43.6529	0.59603	0.58713
300	17.72	44.132	45.8067	45.384	43.6529	0.60343	0.5838
310	17.71	44.142	45.787	45.364	43.6629	0.6143	0.59397
320	17.7	44.082	45.7478	45.374	43.6629	0.60663	0.59056
330	17.72	44.092	45.7576	45.374	43.6629	0.60671	0.59056
340	17.73	44.152	45.8165	45.404	43.7329	0.60713	0.60491
350	17.71	44.152	45.8067	45.335	43.6729	0.61073	0.60807
360	17.73	44.092	45.7576	45.305	43.6129	0.60671	0.59709
370	17.7	44.092	45.7576	45.276	43.5829	0.60671	0.59689
380	17.71	44.092	45.7576	45.276	43.5829	0.60671	0.59689
390	17.72	44.082	45.7478	45.315	43.6229	0.60663	0.59715
400	17.7	44.072	45.7379	45.266	43.5729	0.60656	0.59682
410	17.68	44.062	45.7379	45.266	43.5629	0.60294	0.59332
420	17.69	44.112	45.787	45.296	43.5829	0.60329	0.59005

Table 21 Thermal conductivity data of the composite containing 30% aluminium

Time	T _{ambient}	T ₄	T ₅	T ₇	T ₈	k ₁	k ₂
1	18.41	32.9116	40.4084	33.307	40.8933	0.14712	0.13812
10	18.36	44.4207	53.639	44.954	54.2827	0.11965	0.11232
20	18.35	49.6548	51.254	50.3	51.869	0.68969	0.66796
30	18.32	48.9084	49.978	49.593	50.5778	1.03121	1.06425
40	18.29	48.4174	49.5952	49.095	50.1904	0.93646	0.95686
50	18.27	48.0345	49.2124	48.707	49.803	0.9363	0.95602
60	18.25	47.7202	48.9573	48.341	49.5447	0.89161	0.87019
70	18.22	47.5827	48.8198	48.201	49.4057	0.89156	0.87004
80	18.19	47.1801	48.4174	47.799	49.0139	0.89141	0.86232
90	18.18	46.9935	48.231	47.604	48.8097	0.89134	0.86939
100	18.15	46.7873	47.9758	47.396	48.5515	0.92807	0.90651
110	18.14	46.6695	47.8482	47.276	48.4223	0.93575	0.91423
120	18.12	46.4043	47.6519	47.008	48.2237	0.88411	0.86165
130	18.11	46.149	47.4458	46.772	48.0151	0.85056	0.84295
140	18.1	46.0901	47.3869	46.735	47.9555	0.85054	0.85879
150	18.08	45.9526	47.2495	46.573	47.8164	0.8505	0.84268
160	18.07	45.8151	47.0728	46.434	47.6377	0.877	0.8703
170	18.06	45.6777	46.9256	46.294	47.4887	0.88385	0.87733
180	18.05	45.5009	46.798	46.115	47.3595	0.85034	0.84207
190	18.05	45.3732	46.6802	45.986	47.2403	0.84392	0.83523
200	18.05	45.2456	46.5526	45.856	47.1112	0.84387	0.83506
210	18.04	45.1867	46.425	45.842	47.0371	0.89067	0.8767
220	18.03	45.1081	46.3563	45.757	46.953	0.88364	0.87606
230	18.02	45.0394	46.2876	45.692	46.8976	0.88362	0.86943
240	18	44.9608	46.2091	45.61	46.818	0.88359	0.86724
250	17.99	44.8724	46.1207	45.521	46.7371	0.88355	0.86187
260	17.98	44.8037	46.052	45.453	46.6684	0.88353	0.86235
270	17.97	44.7546	45.9931	45.404	46.5988	0.89051	0.87665
280	17.96	44.6858	45.9244	45.334	46.5291	0.89049	0.87664
290	17.95	44.6957	45.9342	45.344	46.539	0.89049	0.87664
300	17.94	44.5975	45.8263	45.244	46.4329	0.89757	0.88144
310	17.93	44.5385	45.787	45.184	46.3896	0.88343	0.86938
320	17.93	44.4894	45.7379	45.178	46.3838	0.88342	0.86881
330	17.92	44.4796	45.7183	45.125	46.3199	0.89041	0.87661
340	17.92	44.4698	45.7085	45.124	46.31	0.89041	0.88318
350	17.91	44.46	45.7085	45.118	46.31	0.8834	0.87909
360	17.9	44.4403	45.6889	45.089	46.29	0.8834	0.87277
370	17.9	44.4011	45.6496	45.045	46.2502	0.88338	0.86936
380	17.9	44.3225	45.5711	44.991	46.1974	0.88335	0.86878
390	17.89	44.3323	45.5711	44.991	46.1705	0.89036	0.88859
400	17.89	44.3225	45.5613	44.965	46.1605	0.89035	0.87659
410	17.88	44.3225	45.5613	44.965	46.1605	0.89035	0.87659
420	17.87	44.2538	45.4926	44.895	46.0908	0.89033	0.87659

Table 22 Thermal conductivity data of the composite containing 40% aluminium

Time	T _{ambient}	T ₄	T ₅	T ₇	T ₈	k ₁	k ₂
1	20.03	38.5778	43.2351	42.9789	38.5017	0.1959	0.20606
11	20.43	49.8806	56.0535	55.8089	50.2093	0.1478	0.16476
20	20.87	57.7366	59.9795	59.9121	58.07	0.40679	0.50083
30	20.79	56.4699	57.2313	57.3402	56.647	1.19824	1.3309
40	20.64	55.37	56.1909	56.1819	55.4007	1.11146	1.18098
50	20.53	54.3193	55.1309	55.0726	54.2918	1.12416	1.18144
60	20.46	53.4158	54.2377	54.1695	53.4478	1.1101	1.27823
70	20.41	52.424	53.2464	53.1683	52.4468	1.10941	1.27873
80	20.37	51.6089	52.3827	52.3143	51.593	1.17918	1.27915
90	20.34	50.8135	51.5779	51.5682	50.857	1.19369	1.29717
100	20.31	50.0672	50.8908	50.8222	50.0425	1.10779	1.18323
110	20.31	49.3503	50.1154	50.1056	49.3849	1.19252	1.28024
120	20.29	48.7317	49.4971	49.4872	48.7667	1.19203	1.28054
130	20.29	48.1425	48.9082	48.8982	48.1877	1.19156	1.29853
140	20.27	47.5827	48.2898	48.2797	47.6185	1.29031	1.39522
150	20.26	47.0328	47.8678	47.8576	47.0787	1.0927	1.18448
160	20.25	46.6106	47.377	47.3668	46.6273	1.19034	1.24758
170	20.23	46.0508	46.8765	46.8073	46.0091	1.10502	1.15579
180	20.22	45.8053	46.5722	46.503	45.7441	1.1897	1.21571
190	20.21	45.3732	46.1404	46.13	45.3614	1.18935	1.20035
200	20.17	45.0983	45.8655	45.8551	45.0866	1.18913	1.20047
210	20.16	44.7349	45.4926	45.4821	44.7235	1.20425	1.21616
220	20.14	44.4109	45.1883	45.1778	44.3996	1.17358	1.18562
230	20.13	44.1654	44.9331	44.8637	44.0954	1.18839	1.2009
240	20.12	43.8511	44.6289	44.6182	43.8403	1.17315	1.18585
250	20.11	43.6056	44.3737	44.363	43.5949	1.18795	1.20111
260	20.12	43.3798	44.1479	44.1372	43.3692	1.18777	1.20121
270	20.13	43.1539	43.9124	43.8428	43.0846	1.20296	1.21689
280	20.12	42.9084	43.667	43.7151	42.957	1.20276	1.21695
290	20.11	42.7709	43.5394	43.4697	42.7019	1.18729	1.2015
300	20.09	42.5745	43.3431	43.3323	42.5645	1.18713	1.20156
310	20.08	42.4371	43.2057	43.1949	42.4271	1.18702	1.20162
320	20.07	42.3094	43.0781	43.0182	42.2505	1.18692	1.2017
330	20.06	42.1916	42.9603	42.9495	42.1818	1.18683	1.20173
340	20.06	42.0148	42.7836	42.7433	41.9757	1.18669	1.20182
350	20.06	41.9068	42.6659	42.6648	41.907	1.20195	1.21742
360	20.05	41.7693	42.5284	42.547	41.7892	1.20183	1.21747
370	20.03	41.7398	42.5088	42.4685	41.7009	1.18647	1.20194
380	20.05	41.5729	42.342	42.3507	41.5831	1.18634	1.20199
390	20.01	41.5434	42.3223	42.2525	41.4752	1.17137	1.18686
400	20	41.4747	42.2536	42.1642	41.3869	1.17131	1.18689
410	19.98	41.3765	42.1555	42.1445	41.3672	1.17124	1.1869
420	19.96	41.3667	42.1457	42.0758	41.2985	1.17123	1.18693

Table 23 Thermal conductivity data of the composite containing 10% Al(OH)₃

Time	T _{ambient}	T ₄	T ₅	T ₇	T ₈	k ₁	k ₂
1	18.28	21.6776	25.7939	24.8089	20.7409	0.27769	0.2818
10	18.57	32.5876	47.593	44.5005	28.1109	0.06892	0.07731
20	19	38.8233	48.2506	46.2772	36.2758	0.11295	0.12305
30	19.19	39.7857	44.5601	43.7151	38.847	0.23204	0.24296
40	19.28	40.2963	43.6375	43.1458	39.7204	0.32978	0.34718
50	19.37	40.6891	43.667	43.1752	40.1718	0.37611	0.38954
60	19.39	40.9346	43.8044	43.3716	40.427	0.38363	0.40421
70	19.4	41.2488	44.0498	43.617	40.7901	0.3996	0.41415
80	19.36	41.4354	44.2461	43.7544	40.8686	0.39144	0.41272
90	19.37	41.7006	44.5601	44.0096	41.1238	0.39143	0.40565
100	19.35	41.8577	44.6485	44.2256	41.2808	0.3836	0.41565
110	19.31	42.113	44.9724	44.4808	41.477	0.37607	0.40568
120	19.29	42.2701	45.0705	44.579	41.585	0.3773	0.41422
130	19.29	42.388	45.2472	44.7066	41.7518	0.38231	0.4057
140	19.26	42.5451	45.4533	44.9127	41.9088	0.37605	0.39887
150	19.26	42.7317	45.6398	45.0894	42.1542	0.38485	0.39888
160	19.24	42.8888	45.8067	45.1974	42.3112	0.39139	0.39755
170	19.21	43.0459	45.9539	45.3447	42.3505	0.37727	0.3989
180	19.17	43.1048	45.9048	45.4232	42.3603	0.36881	0.41429
190	19.15	43.2128	46.0618	45.5214	42.5271	0.37726	0.40716
200	19.13	43.3798	46.2385	45.6882	42.6841	0.37603	0.40577
210	19.12	43.3601	46.2876	45.7373	42.6743	0.3688	0.39625
220	19.13	43.4387	46.2876	45.7471	42.8019	0.38354	0.40718
230	19.13	43.5565	46.4152	45.9336	42.8608	0.36761	0.40579
240	19.16	43.5173	46.3759	45.8355	42.8313	0.37602	0.40578
250	19.16	43.5762	46.4348	45.8944	42.8804	0.37479	0.40579
260	19.16	43.6449	46.4937	45.9435	42.9393	0.37602	0.40719
270	19.17	43.7137	46.5722	46.022	43.0178	0.37601	0.4058
280	19.18	43.7824	46.6311	46.022	43.0276	0.37725	0.4072
290	19.2	43.7333	46.5918	45.9827	43.0472	0.38482	0.4058
300	19.21	43.694	46.6115	46.0514	42.9982	0.36997	0.39761
310	19.23	43.7137	46.5722	46.0711	43.0767	0.37725	0.4058
320	19.25	43.7922	46.6409	46.0318	43.0963	0.38481	0.4072
330	19.26	43.802	46.7194	46.1692	43.165	0.37601	0.39761
340	19.28	43.7529	46.6704	46.1201	43.1257	0.37724	0.39761
350	19.29	43.7628	46.6802	46.13	43.1355	0.37724	0.39761
360	19.31	43.8413	46.6998	46.1496	43.2042	0.38353	0.40581
370	19.32	43.8511	46.6507	46.0416	43.165	0.39269	0.41434
380	19.32	43.802	46.6606	46.0514	43.165	0.39135	0.40581
390	19.34	43.8217	46.6704	46.0711	43.1257	0.38353	0.4072
400	19.36	43.8413	46.7587	46.1496	43.2042	0.38353	0.39762
410	19.37	43.8511	46.7096	46.1496	43.2141	0.38481	0.40581
420	19.44	43.7333	46.5918	46.0514	43.1061	0.38353	0.4058

Table 24 Thermal conductivity data of the composite containing 20% Al(OH)₃

Time	T _{ambient}	T ₄	T ₅	T ₇	T ₈	k ₁	k ₂
1	18.01	23.838	29.0329	28.117	23.6261	0.21351	0.2569
10	18.12	32.3323	49.7915	47.9951	30.741	0.06353	0.06687
20	18.28	40.2865	48.6334	47.7202	38.3367	0.13288	0.12295
30	18.34	41.7202	45.3552	44.7949	40.741	0.30513	0.28459
40	18.36	41.9166	44.4718	44.0489	41.2906	0.43407	0.41826
50	18.32	41.8773	44.3246	43.9507	41.3593	0.45322	0.44519
60	18.3	41.7988	44.1774	43.8624	41.271	0.4663	0.4452
70	18.25	41.6318	44.0007	43.6955	41.1728	0.46821	0.45733
80	18.21	41.6416	44.089	43.774	41.2415	0.45319	0.45555
90	18.16	41.6024	44.04	43.7348	41.1728	0.45501	0.45032
100	18.12	41.6318	44.0007	43.7544	41.1336	0.46821	0.4402
110	18.07	41.5729	44.0203	43.7642	41.163	0.45319	0.44352
120	18.02	41.5238	43.9614	43.6562	41.1434	0.45501	0.45912
130	17.98	41.5533	43.9909	43.7348	41.1532	0.45501	0.4469
140	17.93	41.5631	44.0007	43.6268	41.0649	0.45501	0.45032
150	17.89	41.5238	43.9614	43.6562	41.1041	0.45501	0.45205
160	17.86	41.4256	43.8731	43.5581	40.9962	0.45317	0.45033
170	17.82	41.4452	43.8829	43.5777	41.006	0.455	0.44861
180	17.79	41.4845	43.9222	43.6759	41.0649	0.455	0.44186
190	17.75	41.4943	43.8829	43.5777	41.0649	0.46435	0.45912
200	17.7	41.4551	43.8927	43.5875	40.9962	0.455	0.44521
210	17.65	41.3961	43.9025	43.5385	40.8784	0.44252	0.43372
220	17.6	41.5336	43.9124	43.6661	41.1434	0.46627	0.45733
230	17.55	41.4943	43.932	43.6857	41.1139	0.455	0.4486
240	17.52	41.4649	43.9025	43.6464	41.0452	0.455	0.44353
250	17.49	41.4354	43.8731	43.617	41.0256	0.455	0.44521
260	17.46	41.4649	43.9025	43.5974	41.0256	0.455	0.44861
270	17.43	41.4354	43.932	43.617	40.9471	0.44427	0.43212
280	17.39	41.3274	43.8338	43.5188	40.8686	0.44252	0.43532
290	17.35	41.4158	43.8535	43.6072	40.9962	0.455	0.44186
300	17.31	41.3765	43.8731	43.5581	40.8686	0.44426	0.42897
310	17.27	41.4551	43.9614	43.6562	40.9962	0.44253	0.43371
320	17.23	41.4158	43.9124	43.5974	40.9569	0.44426	0.43694
330	17.19	41.4452	43.9418	43.6366	40.9765	0.44427	0.43371
340	17.16	41.4158	43.9124	43.6661	40.9962	0.44426	0.43212
350	17.15	41.4649	43.9614	43.6562	41.006	0.44427	0.43532
360	17.13	41.4354	43.9418	43.6366	41.006	0.44253	0.43856
370	17.13	41.3863	43.8829	43.5777	40.9373	0.44426	0.43694
380	17.14	41.3176	43.8338	43.5286	40.9177	0.44079	0.44187
390	17.15	41.3078	43.775	43.5286	40.9079	0.44956	0.44021
400	17.15	41.3274	43.8437	43.4697	40.7999	0.44079	0.43212
410	17.12	41.3078	43.824	43.509	40.8392	0.44079	0.43212

Table 25 Thermal conductivity data of the composite containing 30% Al(OH)₃

Time	T _{ambient}		T ₄	T ₅	T ₇	T ₈	k ₁	k ₂
1	18.29	25.6252	31.4768	31.7098	26.471	0.17147	0.17505	
10	18.27	35.1211	52.1864	52.2946	33.5663	0.05879	0.04897	
20	18.24	48.1327	67.0659	66.705	44.2042	0.052994	0.040756	
30	18.25	52.424	56.7994	56.2604	48.9737	0.229315	0.12585	
40	18.23	51.8053	54.0414	53.6198	49.7784	0.448711	0.238721	
50	18.21	50.9019	52.8538	52.6087	49.7784	0.514037	0.323998	
60	18.19	49.9886	51.941	51.8038	49.3956	0.513914	0.380803	
70	18.18	49.1343	51.2736	51.0872	48.905	0.46901	0.420224	
80	18.18	48.4174	50.4884	50.3608	48.2965	0.484486	0.444238	
90	18.18	47.7595	49.8995	49.8209	47.7666	0.468856	0.446393	
100	18.18	47.2881	49.4284	49.3595	47.3544	0.468803	0.457345	
110	18.17	46.807	48.9474	48.8687	46.9324	0.468749	0.473603	
120	18.17	46.3258	48.4665	48.3386	46.3927	0.468695	0.47125	
130	18.16	45.9133	48.0445	47.9067	46.0296	0.470807	0.488526	
139	18.15	45.5304	47.6028	47.5337	45.6567	0.48414	0.488553	
140	18.15	45.4027	47.5439	47.4748	45.5291	0.468591	0.471308	
150	18.14	45.167	47.2985	47.1705	45.2935	0.470722	0.488579	
160	18.15	44.8135	46.8863	46.8171	44.8716	0.484055	0.471352	
170	18.17	44.4109	46.4937	46.4146	44.5379	0.481725	0.488634	
180	18.17	44.1752	46.2581	46.1889	44.1748	0.481698	0.455317	
190	18.18	43.8806	45.9637	45.8355	43.9491	0.481663	0.486133	
200	18.18	43.6547	45.787	45.6686	43.7234	0.470551	0.47143	
210	18.19	43.4191	45.5024	45.3643	43.4878	0.481608	0.48871	
220	18.2	43.1932	45.2668	45.2072	43.321	0.483861	0.486178	
230	18.19	43.0066	45.0803	44.952	43.1346	0.483838	0.504574	
240	18.2	42.712	44.7957	44.6673	42.7813	0.481524	0.486217	
250	18.22	42.6138	44.6877	44.6182	42.742	0.483791	0.488764	
260	18.22	42.3683	44.4522	44.3827	42.4967	0.481483	0.486237	
270	18.22	42.329	44.4031	44.2747	42.3887	0.483757	0.486245	
280	18.22	42.2014	44.1676	44.0882	42.2121	0.510305	0.488802	
290	18.22	42.0835	44.0988	43.9704	42.1532	0.497863	0.50465	
300	18.21	41.8282	43.9025	43.774	41.9569	0.483697	0.504665	
310	18.21	41.7693	43.7848	43.6562	41.8293	0.497823	0.501963	
320	18.2	41.6416	43.6572	43.5875	41.7116	0.497807	0.488838	
330	18.19	41.5042	43.5885	43.4599	41.6429	0.481381	0.504689	
340	18.18	41.5042	43.5296	43.4599	41.6331	0.495377	0.501978	
350	18.18	41.4354	43.4609	43.3225	41.4957	0.495369	0.501988	
360	18.18	41.3176	43.3333	43.2636	41.3877	0.497766	0.488862	
370	18.18	41.2587	43.2744	43.2047	41.3289	0.497759	0.488866	
380	18.16	41.1703	43.2548	43.136	41.3092	0.481341	0.502003	
390	18.13	41.1506	43.2351	43.1065	41.2209	0.481339	0.486329	
400	18.11	41.1212	43.2057	43.0869	41.2602	0.481336	0.502006	

Table 26 Thermal conductivity data of the composite containing 40% Al(OH)₃

Time	T _{ambient}	T ₄	T ₅	T ₇	T ₈	k ₁	k ₂
1	18.29	25.5729	26.278	24.8216	24.7483	1.52637	14.175
10	18.41	31.19	47.478	48.302	33.1978	0.06607	0.06876
20	18.65	40.9805	55.2024	55.0164	43.0703	0.07567	0.08694
30	19.01	44.5059	49.7257	49.6567	45.2195	0.20618	0.23406
40	19.17	45.4388	48.2141	48.3216	45.6709	0.38778	0.3918
50	19.28	45.6057	47.851	47.8995	45.72	0.47933	0.47649
60	19.38	45.6745	47.743	47.7916	45.6807	0.52028	0.49201
70	19.45	45.6156	47.6154	47.6738	45.612	0.53814	0.50373
80	19.48	45.6647	47.6056	47.6541	45.6513	0.55448	0.51854
90	19.52	45.5861	47.586	47.6345	45.5139	0.53814	0.48974
100	19.54	45.6745	47.6841	47.7327	45.612	0.53552	0.48973
110	19.66	45.5566	47.5075	47.556	45.4943	0.55167	0.50373
120	19.75	45.5763	47.4584	47.5167	45.455	0.57181	0.50374
130	19.83	45.5861	47.478	47.5756	45.5826	0.56885	0.52109
140	19.91	45.5665	47.5271	47.5658	45.5139	0.54891	0.50614
150	19.93	45.5468	47.429	47.5461	45.4943	0.57181	0.50614
160	19.96	45.5763	47.4093	47.5167	45.5237	0.58712	0.5211
170	19.99	45.4781	47.3602	47.4185	45.4746	0.5718	0.53426
180	20.01	45.5075	47.3897	47.4382	45.4452	0.5718	0.5211
190	20.04	45.4584	47.3995	47.448	45.455	0.55445	0.5211
200	20.05	45.537	47.429	47.5363	45.5335	0.56884	0.51854
210	20.03	45.5959	47.5467	47.5952	45.5924	0.55168	0.51854
220	20	45.7334	47.6743	47.7916	45.7298	0.55449	0.50372
230	19.96	45.7727	47.7823	47.7719	45.8279	0.53554	0.53423
240	19.86	45.812	47.8117	47.8603	45.8083	0.53817	0.50612
250	19.81	45.8316	47.8412	47.9486	45.8279	0.53554	0.48972
260	19.77	45.9102	47.9099	47.9683	45.9653	0.53818	0.51851
270	19.74	45.9298	47.9393	48.0468	45.9849	0.53556	0.5037
280	19.68	46.0084	48.008	48.0664	46.0046	0.5382	0.5037
290	19.62	46.028	48.0866	48.1449	46.0831	0.5228	0.50369
300	19.6	45.9887	48.0473	48.1646	46.1027	0.5228	0.50369
310	19.55	46.0771	48.1454	48.1842	46.1321	0.52033	0.5061
320	19.52	46.0476	48.1062	48.1646	46.1125	0.52281	0.5061
330	19.5	46.028	48.1553	48.1449	46.142	0.50592	0.5185
340	19.45	46.0575	48.116	48.2235	46.1125	0.52281	0.49198
350	19.41	46.0967	48.224	48.2627	46.2106	0.50593	0.50609
360	19.33	46.1655	48.2927	48.4002	46.2793	0.50593	0.48969
370	19.31	46.2146	48.3417	48.3904	46.3284	0.50594	0.50368
380	19.26	46.2735	48.4006	48.5082	46.3971	0.50595	0.49196
390	19.25	46.2637	48.4497	48.4983	46.3775	0.49232	0.48969
400	19.23	46.303	48.4301	48.5376	46.4265	0.50595	0.49196
410	19.2	46.3324	48.5086	48.5572	46.3873	0.49455	0.47861
420	19.19	46.2539	48.3712	48.4787	46.3677	0.50829	0.49196

Table 27 Thermal conductivity data of the composite containing 10% graphite

Time	T _{ambient}	T ₄	T ₅	T ₇	T ₈	k ₁	k ₂
1	19.71	37.5467	47.4556	47.2588	37.1983	0.09838	0.0969
10	19.66	43.4479	53.6488	54.2383	43.6262	0.09556	0.09186
20	19.6	45.7561	50.7338	50.9105	45.5301	0.19584	0.18118
30	19.56	46.0664	49.6345	49.6835	45.9717	0.27321	0.26263
40	19.53	45.9791	49.1143	49.2319	45.9913	0.31094	0.30082
50	19.49	45.6979	48.7315	48.8295	45.7754	0.32134	0.31919
60	19.47	45.3875	48.4076	48.584	45.5202	0.32279	0.31818
70	19.43	45.116	48.1328	48.3092	45.3044	0.32313	0.32442
80	19.4	45.3634	47.9169	48.0343	45.0296	0.38177	0.32443
90	19.38	44.6505	47.6617	47.7791	44.7744	0.32374	0.32444
100	19.37	44.4759	47.4359	47.6024	44.5978	0.32933	0.32444
110	19.35	44.2141	47.1611	47.3276	44.323	0.33078	0.32445
120	19.33	44.0201	46.9059	47.1312	44.1365	0.3378	0.32552
130	19.36	43.8067	46.7489	46.9742	44.0384	0.33133	0.33205
140	19.34	43.7388	46.6213	46.8564	43.9108	0.3382	0.33095
150	19.33	43.4867	46.425	46.6502	43.6557	0.33177	0.32553
160	19.31	43.4673	46.3563	46.5128	43.5772	0.33743	0.33207
170	19.28	42.769	46.1404	46.4343	43.4888	0.28915	0.33096
180	19.26	43.1957	46.1305	46.3557	43.3514	0.33216	0.32448
190	19.24	43.1279	46.0422	46.2674	43.2631	0.33449	0.32448
200	19.2	43.0697	45.9441	46.179	43.1748	0.33914	0.32449
210	19.17	42.9824	45.9244	46.0907	43.1454	0.33135	0.33097
220	19.14	42.8272	45.7674	45.9925	42.9883	0.33156	0.32449
230	19.11	42.7399	45.6692	45.9631	42.8902	0.33279	0.31724
240	19.12	42.6914	45.6791	45.8551	42.8509	0.32629	0.32449
250	19.09	42.672	45.5416	45.8355	42.8313	0.33971	0.3245
260	19.06	42.6332	45.5024	45.7373	42.7332	0.33977	0.3245
270	19.03	42.6042	45.4729	45.7668	42.7037	0.33981	0.31826
280	18.99	42.5169	45.4435	45.7275	42.6645	0.33309	0.31826
290	18.96	42.6042	45.5318	45.7569	42.6939	0.33297	0.31826
300	18.93	42.5169	45.4435	45.7275	42.6645	0.33309	0.31826
310	18.9	42.4878	45.4729	45.698	42.635	0.32656	0.31826
320	18.87	42.4587	45.3846	45.6784	42.6743	0.33317	0.3245
330	18.84	42.4296	45.3552	45.6391	42.586	0.33321	0.31929
340	18.81	42.4102	45.3355	45.6195	42.5565	0.33324	0.31826
350	18.79	42.3229	45.2963	45.5312	42.4682	0.32785	0.31827
360	18.75	42.3423	45.2668	45.4919	42.4388	0.33333	0.31929
370	18.73	42.3229	45.257	45.541	42.478	0.33224	0.31827
380	18.71	42.3035	45.2276	45.5115	42.4486	0.33338	0.31827
390	18.69	42.2841	45.2668	45.4919	42.429	0.32683	0.31827
400	18.66	42.255	45.2374	45.4723	42.4093	0.32687	0.31827
410	18.64	42.2841	45.2766	45.5017	42.3799	0.32576	0.31226
420	18.61	42.2647	45.257	45.4723	42.3897	0.32578	0.31624

Table 28 Thermal conductivity data of the composite containing 20% graphite

Time	T _{ambient}	T ₄	T ₅	T ₇	T ₈	k ₁	k ₂
1	18.4	23.4399	24.145	22.6886	22.6153	1.53407	14.5438
10	18.51	29.057	46.052	46.876	31.0648	0.06364	0.06739
20	18.82	38.8475	53.7764	53.5904	40.9373	0.07245	0.08421
30	19.12	42.3729	48.2997	48.2307	43.0865	0.1825	0.20714
40	19.28	43.3058	46.7881	46.8956	43.5379	0.31061	0.31735
50	19.39	43.4727	46.425	46.4735	43.587	0.36638	0.36915
60	19.47	43.5415	46.317	46.3656	43.5477	0.38971	0.37815
70	19.53	43.4826	46.1894	46.2478	43.479	0.39959	0.38486
80	19.57	43.5317	46.1796	46.2281	43.5183	0.40848	0.39322
90	19.62	43.4531	46.16	46.2085	43.3809	0.39959	0.37685
100	19.65	43.5415	46.2581	46.3067	43.479	0.39815	0.37684
110	19.71	43.4236	46.0815	46.13	43.3613	0.40697	0.38486
120	19.79	43.4433	46.0324	46.0907	43.322	0.41777	0.38487
130	19.86	43.4531	46.052	46.1496	43.4496	0.41619	0.39465
140	19.91	43.4335	46.1011	46.1398	43.3809	0.40547	0.38623
150	19.95	43.4138	46.003	46.1201	43.3613	0.41776	0.38623
160	19.98	43.4433	45.9833	46.0907	43.3907	0.42584	0.39466
170	20	43.3451	45.9342	45.9925	43.3416	0.41776	0.40197
180	20.03	43.3745	45.9637	46.0122	43.3122	0.41776	0.39466
190	20.04	43.3254	45.9735	46.022	43.322	0.40847	0.39466
200	20	43.404	46.003	46.1103	43.4005	0.41619	0.39323
210	19.94	43.4629	46.1207	46.1692	43.4594	0.40697	0.39322
220	19.89	43.6004	46.2483	46.3656	43.5968	0.40849	0.38485
230	19.87	43.6397	46.3563	46.3459	43.6949	0.39816	0.40195
240	19.85	43.679	46.3857	46.4343	43.6753	0.39961	0.38622
250	19.81	43.6986	46.4152	46.5226	43.6949	0.39816	0.37683
260	19.76	43.7772	46.4839	46.5423	43.8323	0.39961	0.39321
270	19.72	43.7968	46.5133	46.6208	43.8519	0.39817	0.38484
280	19.68	43.8754	46.582	46.6404	43.8716	0.39962	0.38484
290	19.64	43.895	46.6606	46.7189	43.9501	0.39111	0.38484
300	19.6	43.8557	46.6213	46.7386	43.9697	0.39111	0.38484
310	19.57	43.9441	46.7194	46.7582	43.9991	0.38973	0.38621
320	19.54	43.9146	46.6802	46.7386	43.9795	0.39112	0.38621
330	19.52	43.895	46.7293	46.7189	44.009	0.38163	0.3932
340	19.48	43.9245	46.69	46.7975	43.9795	0.39112	0.37814
350	19.41	43.9637	46.798	46.8367	44.0776	0.38164	0.3862
360	19.35	44.0325	46.8667	46.9742	44.1463	0.38164	0.37682
370	19.34	44.0816	46.9157	46.9644	44.1954	0.38165	0.38483
380	19.28	44.1405	46.9746	47.0822	44.2641	0.38165	0.37813
390	19.27	44.1307	47.0237	47.0723	44.2445	0.37388	0.37681
400	19.25	44.17	47.0041	47.1116	44.2935	0.38165	0.37812
410	19.21	44.1994	47.0826	47.1312	44.2543	0.37516	0.37039

Table 29 Thermal conductivity data of the composite containing 30% graphite

Time	T _{ambient}	T ₄	T ₅	T ₇	T ₈	k ₁	k ₂
1	18.29	34.4239	50.3608	48.0932	31.6167	0.06507	0.06216
10	18.3	41.4354	47.8678	46.0122	38.1623	0.16122	0.13047
20	18.27	42.6629	45.3944	44.2452	40.2821	0.37965	0.25843
30	18.23	42.8102	44.9527	44.098	41.2144	0.48401	0.35518
40	18.2	42.8397	44.9233	44.2452	41.656	0.49769	0.39556
50	18.15	42.8495	44.992	44.3827	41.9111	0.48401	0.4144
60	18.1	42.8691	45.0607	44.5103	42.1565	0.47318	0.43512
70	18.05	42.8102	45.1294	44.5299	42.2252	0.44714	0.44439
80	18.01	42.8888	45.2079	44.6575	42.3724	0.44715	0.4482
90	17.98	43.0459	45.365	44.8146	42.4607	0.44716	0.43511
100	17.92	43.1146	45.3748	44.8931	42.5883	0.45882	0.44437
110	17.9	43.0754	45.4533	44.844	42.5588	0.43609	0.44819
120	17.88	43.1736	45.5613	45.0207	42.7159	0.43431	0.44436
130	17.85	43.1441	45.4631	44.9815	42.6864	0.44717	0.44626
140	17.83	43.2619	45.5809	45.0305	42.7944	0.44718	0.45801
150	17.82	43.1736	45.6104	45.0698	42.7159	0.42556	0.43509
160	17.81	43.2914	45.7281	45.1287	42.8336	0.42557	0.44625
170	17.8	43.2816	45.6594	45.1778	42.8238	0.43611	0.43509
180	17.8	43.2227	45.6104	45.1091	42.7649	0.43431	0.43691
190	17.8	43.3405	45.7183	45.1778	42.8827	0.43612	0.44625
200	17.78	43.2619	45.6496	45.0993	42.8042	0.43432	0.44626
210	17.78	43.2521	45.6889	45.0894	42.8532	0.42557	0.45801
220	17.77	43.3209	45.6987	45.0894	42.8631	0.43611	0.46003
230	17.76	43.3601	45.7968	45.1974	42.9023	0.42558	0.44625
240	17.74	43.3405	45.7183	45.1778	42.8827	0.43612	0.44625
250	17.72	43.3209	45.7085	45.168	42.8729	0.43432	0.44625
260	17.71	43.3798	45.7576	45.217	42.8631	0.43612	0.43509
270	17.7	43.311	45.7478	45.2072	42.9121	0.42557	0.44625
280	17.71	43.37	45.7478	45.2563	42.9023	0.43612	0.43509
290	17.69	43.3012	45.7674	45.1974	42.9023	0.42049	0.44625
300	17.69	43.3601	45.8067	45.1974	42.9023	0.42387	0.44625
310	17.7	43.37	45.787	45.2661	42.9121	0.42903	0.43508
320	17.7	43.311	45.7478	45.2072	42.9121	0.42557	0.44625
330	17.72	43.3209	45.7576	45.2072	42.9121	0.42557	0.44625
340	17.72	43.3798	45.8165	45.2759	42.9808	0.42558	0.44625
350	17.71	43.3798	45.8067	45.2661	42.9219	0.4273	0.43691
360	17.72	43.3209	45.7576	45.2072	42.8631	0.42557	0.43691
370	17.72	43.3209	45.7576	45.2661	42.8336	0.42557	0.42104
380	17.71	43.3209	45.7576	45.217	42.8336	0.42557	0.42971
390	17.71	43.311	45.7478	45.2563	42.8729	0.42557	0.42971
400	17.7	43.3012	45.7379	45.1876	42.8238	0.42557	0.43328
410	17.69	43.2914	45.7379	45.2465	42.814	0.42386	0.42104

Table 30 Thermal conductivity data of the composite containing 40% graphite

Time	T _{ambient}	T ₄	T ₅	T ₇	T ₈	k ₁	k ₂
1	17.38	41.8567	44.6583	44.5299	41.3495	0.35417	0.32422
10	17.34	41.8763	44.2559	44.1372	41.6733	0.41699	0.4185
20	17.29	42.004	44.2755	44.1372	41.8009	0.43682	0.44135
30	17.26	42.1611	44.3639	44.2354	42.0659	0.45046	0.47528
40	17.24	42.3182	44.5798	44.4514	42.2229	0.43875	0.46271
50	17.2	42.3968	44.6092	44.471	42.2425	0.44849	0.46271
60	17.17	42.495	44.7564	44.6771	42.3406	0.43876	0.44132
70	17.14	42.5343	44.8546	44.7459	42.3799	0.42763	0.43583
80	17.11	42.6128	44.884	44.8048	42.4584	0.43688	0.43947
90	17.09	42.711	44.9822	44.9127	42.5664	0.43689	0.43946
100	17.07	42.8191	45.0803	45.0109	42.6645	0.43879	0.43946
110	17.05	42.9271	45.1883	45.1287	42.7724	0.43881	0.43762
120	17.04	43.0253	45.2963	45.1778	42.8706	0.43692	0.44693
130	17.01	43.0547	45.3257	45.2269	42.9098	0.43692	0.44503
140	17	43.1038	45.365	45.2956	42.9491	0.43882	0.43944
150	16.97	43.0744	45.3944	45.2759	42.9196	0.42768	0.43761
160	16.96	43.1726	45.3748	45.2465	42.9687	0.45056	0.4527
170	16.94	43.2119	45.4828	45.3447	43.008	0.43694	0.44129
180	16.92	43.3199	45.522	45.4526	43.1159	0.45058	0.44128
190	16.9	43.2511	45.5613	45.4428	43.0865	0.42952	0.43761
200	16.89	43.2904	45.6104	45.4625	43.0668	0.4277	0.43043
210	16.88	43.3395	45.5907	45.4723	43.1257	0.44076	0.43943
220	16.87	43.3297	45.6496	45.5214	43.1748	0.42771	0.43943
230	16.85	43.369	45.6889	45.5017	43.165	0.42771	0.44128
240	16.84	43.4279	45.6889	45.5606	43.2729	0.43886	0.45074
250	16.83	43.4083	45.7379	45.6097	43.2631	0.42591	0.43943
260	16.81	43.4574	45.7183	45.6097	43.3024	0.43886	0.4469
270	16.81	43.4868	45.7183	45.649	43.3024	0.44465	0.43943
280	16.8	43.5065	45.7576	45.6882	43.2827	0.44078	0.42867
290	16.79	43.5261	45.7478	45.6784	43.2729	0.44662	0.42867
300	16.78	43.5457	45.8655	45.7275	43.322	0.42773	0.42867
310	16.76	43.5261	45.8459	45.7275	43.3809	0.42772	0.43942
320	16.75	43.5752	45.8459	45.7569	43.3024	0.43697	0.42009
330	16.74	43.5654	45.8263	45.7962	43.3514	0.43887	0.42178
340	16.73	43.6145	45.8754	45.7471	43.3416	0.43887	0.42866
350	16.72	43.6047	45.9244	45.806	43.4005	0.42773	0.42866
360	16.72	43.7323	45.9931	45.8649	43.4594	0.43889	0.42866
370	16.7	43.6341	45.9048	45.8355	43.43	0.43698	0.42866
380	16.69	43.7029	45.9637	45.8944	43.4888	0.43888	0.42866
390	16.69	43.7029	45.9637	45.8944	43.4888	0.43888	0.42866
400	16.69	43.7029	45.9637	45.8355	43.4201	0.43888	0.42692
410	16.67	43.6243	45.9244	45.8158	43.4103	0.43138	0.42866

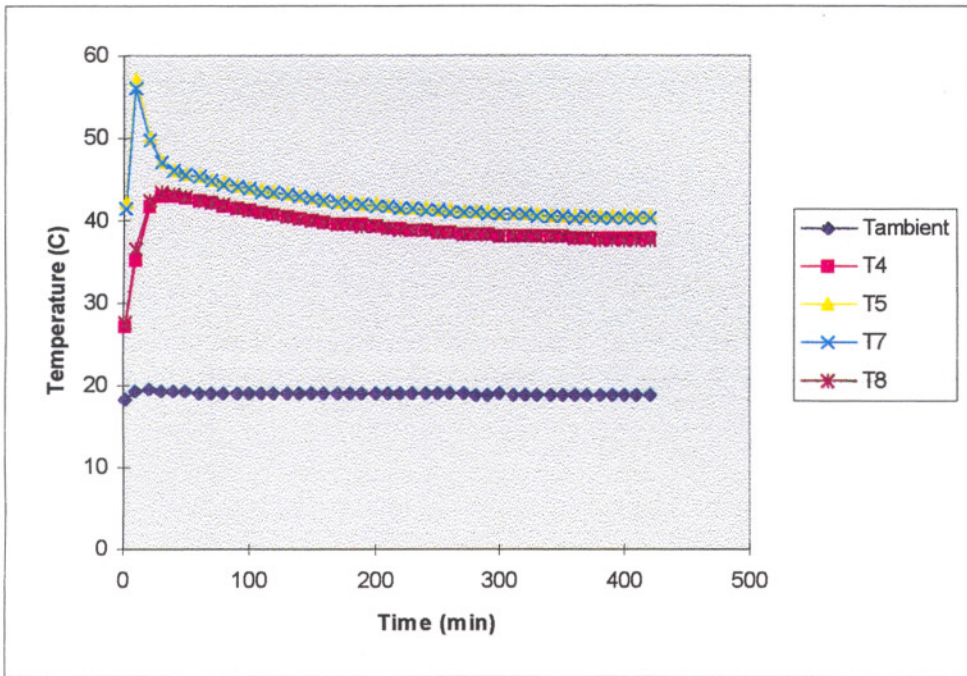


Figure 26 Temperature variation with respect to time for the clinoptilolite

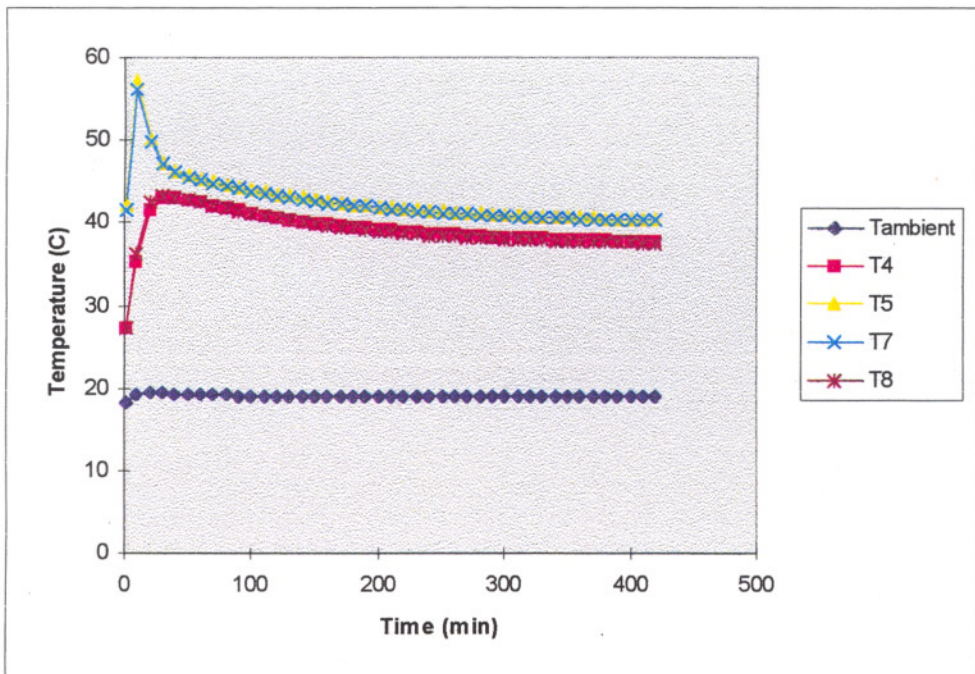


Figure 27 Temperature variation with respect to time for the clinoptilolite containing polyvinylalcohol